




Rico Lead (Pb) Micromineralogy Study Rico, Colorado

Prepared for:

**Titan Environmental Corporation
7939 East Arapahoe Road
Suite 230
Englewood, Colorado 80112**

April 12, 1996


Geomega

RICO LEAD (Pb) MICROMINERALOGY STUDY RICO, COLORADO

1.0 Introduction

This research uses electron microprobe analysis (EMPA) to determine the micromineralogy of Pb-bearing geologic materials collected in Rico, Colorado. EMPA provides elemental chemical analysis of complex Pb solid phases that is not attainable by traditional optical and x-ray diffraction methods. In this context, the term "micromineralogy" refers to micron-scale Pb mineral morphology generated by solid solution phases, pedogenic reactions, and secondary precipitation/dissolution reactions that are visible and/or quantifiable using electron microprobe techniques.

Thirteen (13) samples of bedrock and surficial materials from Rico, Colorado were analyzed using EMPA. Field lithologic descriptions of the samples are provided in Table 1. Samples were preliminarily subdivided into six groups based on common origin of materials to facilitate interpretation of EMPA results as follows: 1) bedrock outcrops (n=3); 2) colluvium (n=3); 3) alluvium (n=3); 4) roadfill material (n=2); 5) one sample from the former Grandview Smelter site; and 6) one sample of waste rock from the Van Winkle mine site.

Materials and methods used for the EMPA analysis are presented in Section 2. EMPA results given by frequency of occurrence and relative Pb mass of observed Pb phases are presented in Section 3, in addition to a discussion of probable geochemical reactions controlling the observed Pb phases in each sample group. Representative photomicrographs of important Pb phases are provided for selected samples.

2.0 Materials and Methods

Sample Preparation and Analysis. Samples were prepared for EMPA analysis by drying and sieving to <250 μm , and by embedding 4 g of sample in epoxy within a sample mold. The molds were set to cure at room temperature, and a flat surface was ground to expose as much sample as possible. Successive polishing steps employed a 600-grit wet/dry abrasive paper stretched across a glass plate, 15- μm and 6- μm diamond on a cloth pad fixed to a

steel lap, and finally 0.1- μm diamond on a felt pad fixed to a steel lap. All polishing steps used kerosene to avoid dissolution of water-soluble Pb phases, and all polishing was performed at low speeds to avoid plucking of the sample grains. Finally, sample pucks were cleaned in an ultrasonic cleaner with isopropyl alcohol, air dried, and placed in a carbon coater, where a thin layer of carbon was sputtered onto the surface of each puck. In addition to EMPA analysis, the pH of each sample was measured using the saturated paste method (Black 1965). Total Pb concentrations were measured by inductively coupled plasma spectroscopy (ICP).

EMPA Parameters. EMPA analysis was conducted at the Laboratory for Geological Studies, University of Colorado, Boulder, on a JEOL 8600 electron microprobe operating at 15 kV with a 20-nA specimen current and a 1- μm beam. Quantitative data were collected using wavelength dispersive spectrometers and mineral standards, and corrected using Phi Rho Z parameters. The Pb-bearing particles were identified using a combination of energy dispersive detection (EDS), wavelength dispersive detection (WDS), and backscatter electron image detection (BEI). Initially spectra are generated for each grain that allow identification of all elements with an atomic mass greater than or equal to carbon. Subsequently, the elemental proportions are quantified using standards, and the mineral is identified based on the equivalent weight of the oxide. Therefore, the identifications provide quantitative stoichiometric ratios from which the mineral identity can be calculated. The relations between Pb-bearing phases were established from BEI images and WDS/EDS analyses as necessary. Representative BEI photomicrographs of identified phases and their associations were produced, with scale bar, magnification, sample identification, and phase identification recorded on each photomicrograph.

Point Count Analysis. Individual Pb-bearing particles were analyzed (representing one point count each) until a minimum of 100 particles had been evaluated. Point counts were made by traversing each sample from left to right and top to bottom in a grid pattern, with each vertical displacement moving only to the adjacent field of view. Magnification settings of 40 to 100 \times and 300 to 600 \times were used; the latter magnification allowed analysis of the smallest identifiable phases (1–2 μm). The grain size of each Pb carrier was determined by measuring the dimension of the long axis. Percent compositions of Pb phases in each

sample were determined by summing the total area of all Pb grains and dividing the area for each phase by the total sample area. The overall frequency of Pb phases present in the Rico samples was calculated by summing the total number of each Pb phase (weighted for grain size), and normalizing the total to 100%. The observed physical associations (liberated, included, etc.) of Pb phases as determined by EMPA following the method of Link et al. (1994).

3.0 Results and Discussion

EMPA results showing the observed types and frequency of occurrence and relative Pb mass of Pb phases in Rico samples are presented in Table 2. Proposed mineral reactions controlling the occurrence of Pb phases are listed in Table 3, and the physical associations of Pb phases are presented in Table 4. A ternary diagram showing the relationship of individual samples to the four mineral assemblages is presented in Figure 1. Frequency of occurrence of Pb phases for the six sample groups are summarized in Figures 2 through 6, while results for individual samples are graphically illustrated in Figures 7 through 19. Selected photomicrographs showing the relationship of important Pb phases are shown in Figures 20 through 22.

Results indicate the presence of four Pb phase assemblages consisting of: 1) a primary mineral phase assemblage represented by galena (PbS), 2) a secondary assemblage consisting of cerussite (PbCO₃) and anglesite (PbSO₄); 3) a tertiary mineral assemblage consisting of poorly crystallized and compositionally-variable Pb-bearing Fe- and Mn-oxides, Pb-bearing Fe- and Mn-silicates, and Pb organics, which are derived principally from the alteration of primary and secondary Pb phases; and 4) particles of slag, solder, Pb-metal oxides (Pb[M]O; where M=Cu, Ni, etc.), and Pb-based paint, which are classified as anthropogenically-derived Pb phases. These assemblages and individual sample results are graphically illustrated on the ternary diagram of Figure 1.

EMPA results indicate a high proportion of primary (PbS) and secondary (PbSO₄ and PbCO₃) phases present in bedrock samples with minor amounts of tertiary phases and an absence of anthropogenic phases (Figure 2). The number of tertiary phases (primarily Pb-bearing Fe-

and Mn-oxides) increase in alluvium and colluvium samples accompanied by a corresponding decrease in primary and secondary phases (Figure 3). Slag is dominant in the sample from the Grandview Smelter site (Figure 4); while roadfill samples have a mineral assemblage similar to the alluvial/colluvial samples, i.e., dominated by tertiary phases but also containing primary and secondary phases and slag (Figure 5). The Van Winkle mine site sample is composed of a roughly equal mix of primary, secondary, and tertiary oxide phases (Figure 6).

The existence of the observed mineral assemblages is the result of a sequence of near-surface geochemical reactions that alter relatively unstable primary and secondary minerals to more stable tertiary phases. The primary assemblage (PbS) represents the original form of Pb produced under sulfide-rich, geochemically-reducing conditions (sulfide ore formation) in the Rico area (McKnight 1974). Alteration of PbS occurs after exposure to cool, moist, oxygenated surface conditions and results in the formation of the secondary assemblage, represented by the minerals PbSO_4 and PbCO_3 . Alteration of the secondary assemblage phases produces a tertiary assemblage represented by complex oxide, silicate, phosphate, and sulfate phases. Minor anthropogenic input from local smelters, mines, and other human activities have introduced artificial phases such as slag (complex metal silicates), solder, and paint.

Surficial chemical weathering of liberated galena (galena that is free from encapsulation by other mineral phases and therefore susceptible to weathering) provides the ultimate source of Pb for the subsequent formation of secondary and tertiary Pb phases according to the reactions outlined in Table 3. Lead released by oxidation of PbS and dissolution of PbSO_4 and PbCO_3 is scavenged by Fe and Mn oxides by adsorption and coprecipitation reactions that result in the formation of a series of poorly crystallized FePb oxide and MnPb oxide solids with highly variable Pb content. Lead-bearing Fe oxide and Mn oxide phases may range in composition from nearly pure end-members (e.g., FeOOH , Fe_2O_3 , MnO_2) to impure solid solution species represented by FePb- and MnPb-oxides of highly variable composition and which are typically amorphous. Dissolution of pyrite, hematite, chlorite, hornblende, siderite and other Fe-bearing minerals provide dissolved Fe from which FePb-oxide and FePb-silicate solids are formed. Oxidation of pyrite (FeS_2), which is ubiquitous in the Rico ores

(McKnight 1974), provides a source of dissolved Fe and decreases local system pH which acts to increase the solubility of Pb^{+2} . Acid generation by pyrite is buffered by the presence of abundant carbonates in the area. Manganese derived from alteration and dissolution of $MnCO_3$ (rhodochrosite), $MnSiO_3$ (rhodonite), and other gangue minerals provides a source of Mn ions. Mn complexes strongly with Pb and forms several crystalline and amorphous MnPb oxides of variable Pb content (Davis et. al 1993). Dissolved silica (H_4SiO_4) complexes with Fe and Pb to form FePb silicates, probably as $(Fe,Pb)SiO_3$ and as Pb_2SiO_4 . The small occurrence of Pb phosphate phases in the Rico samples is probably due to insufficient soil PO_4 in Rico alluvial/colluvial materials. The lack of FePb sulfate minerals (such as plumbojarosite) is probably due to the near neutral to slightly alkaline pH's of most samples which prevent the formation of these phases in any quantity. Many of the Pb-bearing phases observed in the Rico samples appear similar in composition to the Pb-bearing ores of the Butte district, Montana, as described by Davis et al. (1993), and the reader is referred to that report for additional description of Pb phase mineralogy and geochemistry.

3.1 Bedrock Outcrop Samples

EMPA results for Rico bedrock outcrop samples (samples 906, 910, and 917) are listed in Table 2 and the frequency of occurrence of observed phases are summarized in Figure 2. Results show that primary and secondary assemblage minerals are the dominant Pb phases in Rico bedrock samples. As a group, the dominant phases consist of cerussite (frequency of occurrence = 46%), anglesite (23%) and galena (20%). Subordinate phases include FePb oxide (9%), MnPb oxides (<2%), and Pb phosphates (<1%). The cumulative Pb mineralogy for bedrock samples is cerussite > anglesite > galena > > FePb oxides > MnPb oxides > Pb phosphates.

3.1.1 Sample 906 (Lab no. S001542)

Sample 906 is described in Table 1 as an 8-ft chip sample of hornblende latite porphyry obtained from a road cut outcrop. Field description of this sample identified it as being strongly chloritized with veinlets of quartz, hematite, pyrite, and galena with a trace of CuO staining. ICP analysis measured 13,600 mg/kg of total Pb; and the measured pH is 6.48 indicating slightly acidic conditions.

EMPA analysis of sample 906 is graphically presented in Figure 7. The most frequently occurring Pb phases in this sample are the primary and secondary phases galena (42%) and anglesite (38%), followed by the tertiary phase FePb oxide (11%). The high proportion of anglesite indicates that galena is being oxidized in situ by oxygen, according to equation (1) in Table 3. Cerussite was detected at a frequency of 7.6%, suggesting that minor carbonate is present in this sample. Both MnPb oxide and Pb phosphate phases occur in trace amounts (<1%) indicating an apparent lack of Mn and PO_4 as well. Over 90% of Pb mass in this sample is contained in two phases: galena (57%) and anglesite (34%), with the remainder of the mass being contained in cerussite (8%) and FePb-oxide (0.6%). Approximately 96% of the Pb phases occur as liberated grains (Table 4), with less than half a percent (0.3%) occurring within ("included") another grain.

3.1.2 Sample 910 (Lab.no. S001546)

Sample 910 is described as a 6-ft chip sample obtained from an outcrop of hornblende latite porphyry. Field observations describe this sample as chloritized and brecciated, with limonite, MnO, and CuO in fractures and in breccia matrix, with some clay altered clasts. Total Pb by ICP is 39,700 mg/kg; and the pH is 6.5.

EMPA analysis of sample 910 is graphically presented in Figure 8. The most frequently occurring Pb phase, and the phase containing the majority of Pb mass in this sample, is cerussite (frequency of occurrence = 81%; relative Pb mass = 90%); suggesting that an abundant source of carbonate is present that prevents the formation of anglesite (see equation [4] in Table 3). Anglesite is the second most abundant Pb phase but is still relatively minor compared to cerussite (frequency = 8%; Pb mass = 7.4%). FePb-oxide is also present (frequency = 6%; Pb mass = 0.4%). Other phases detected by EMPA (galena, MnPb-oxide, and Pb phosphate) are subordinate to cerussite; the combined total of these phases contributes less than 5% of the Pb phase frequency and <2% of the total Pb mass. Of the total Pb phases observed by EMPA, approximately 84% occur as liberated grains with only 5.7% occurring included within other phases.

3.1.3 Sample 917 (Lab no. S001553)

Sample 917 is described as a 6-ft chip sample obtained from the Leadville Limestone from an outcrop located at the caved Shamrock adit portal. Field observations describe this sample as strongly chloritized, vuggy, and containing pods and blebs of pyrite, sphalerite, and galena. Total Pb is 21,200 mg/kg and the sample pH is 6.0. A pH of 6 in this setting (Leadville Limestone) suggests that oxidation of pyrite, and subsequent acid generation, may be significant although it is probably buffered by carbonate soon after being formed.

EMPA analysis of sample 917 is graphically presented in Figure 9. Sample 917 is dominated by primary mineral assemblage phases including cerussite (frequency of occurrence = 48.4%), galena (18.4%), and anglesite (21.9%). The existence of abundant cerussite and anglesite suggest that competing anion ligands (sulfate and carbonate) are present in significant amounts. Lesser amounts of FePb-oxide (10%) and MnPb-oxide (<1%) were also detected. The majority of Pb mass is contained in the cerussite (53%) with roughly equal amounts contained in galena (25.6%) and anglesite (20.3%). Over 95% of Pb phases occur as liberated grains with an equal number occurring as attached, included, and as rims on other grains (Table 4).

3.2 Alluvium and Colluvium Samples

Alluvium and colluvium samples consist of six samples including 932, 938, 939, 940, 943, and 945. These are loosely subdivided into "undisturbed" alluvium (samples 938 and 939); and "disturbed" colluvium (samples 932, 940, 943, and 945) depending on whether or not they are from an area impacted by human activities. The combined bulk Pb phase composition of these samples is illustrated on Figure 3. In contrast to the mineralogy of the bedrock outcrop samples, alluvium/colluvium samples are characterized by a variety of tertiary assemblage minerals, consisting primarily of FePb-silicates (frequency of occurrence = 33%), with lesser amounts of FePb-oxides (17%) and MnPb-oxides (15%), and proportionally lesser amounts of primary and secondary phases. Primary and secondary phases including cerussite (frequency = 8%), galena (2.5%), and anglesite (2.5%). The lack of these phases suggests that significant weathering and alteration have occurred with subsequent redistribution of Pb to the tertiary phases. Other tertiary phases detected include Pb organics (Pb adsorbed to soil organic matter, FePb-sulfates (variation of

FePb-sulfates (variation of plumbojarosite; see equation [12] in Table 3), Pb phosphates, and Pb silicates. Minor amounts of anthropogenic phases including slag, mixed Pb-metal oxides (Pb(M)O), and solder were also found in some samples. The frequency of Pb phases in the alluvium/colluvium samples are FePb-silicate > FePb-oxide > MnPb-oxide > cerussite > galena > anglesite > Pb(M)O > Pb organics > slag > FePb sulfate > Pb phosphate > Pb silicate > solder > clay.

3.2.1 Sample 932 (Lab no. S001568)

Sample 932 is described as dark brown soil, and mixed rock fragments collected from the 3- to 6-inch depth interval in mixed, disturbed colluvium. Total Pb by ICP is 1150 mg/kg and the sample pH is 6.2. EMPA analysis of sample 932 is presented in Table 2 and graphically depicted in Figure 10. Several secondary Pb phases are present in relatively equal amounts in this sample. The most frequent being the tertiary phases FePb oxide (32%), FePb silicate (24.8%), and MnPb oxide (18%). Lesser amounts of Pb organics (8%), Pb(M)O (7.6%), slag (7.2%), and solder (1%) are also present. Galena occurs only in trace amounts (0.1%), but contributes almost 2% of the total Pb mass. Most of the Pb mass is distributed among four phases including Pb(M)O (32%), MnPb oxide (25.4%), FePb oxide (21%), and FePb silicate (18.5%). The presence of Pb(M)O is probably anthropogenic in origin and may represent smelter-derived material (Drexler 1996). Table 4 indicates that 67% of Pb phases occur as "free" or liberated grains, whereas almost 30% occur as attached to non-Pb phases. Only 2% occur included, or within, other grains and < 1% occur as rims.

3.2.2 Sample 938 (Lab no. S001574)

Sample 938 was collected from a utility excavation in undisturbed alluvial material in a Quaternary fan deposit, and is described as unconsolidated, stratified, sand, silt, clay and gravel of mixed composition, and exhibiting graded bedding. Total Pb by ICP is 598 mg/kg with a pH of 6.9. EMPA analysis of sample 938 is presented in Table 2 and graphically presented in Figure 11.

Eight Pb-bearing phases were detected in this sample, the most frequent Pb phases being the tertiary phases FePb oxide (frequency of occurrence = 42%), MnPb oxide (26%), and Pb phosphate (16%). Cerussite and Pb silicate were detected at a frequency of approximately

7%, with galena, anglesite, and solder occurring less than 1%. This assemblage suggests that significant alteration of primary and secondary phases has occurred resulting in the formation of stable tertiary Pb phases probably due to typical pedogenic reactions (Table 3). While cerussite had a frequency of <8%, it contained 34% of the total Pb mass. The remaining 60% of total Pb mass was roughly equally distributed among four phases including Pb silicate (17%), MnPb oxide (16%), Pb phosphate (13.6%), and FePb oxide (11.5%). This shows that while tertiary phases are abundant, the amount of Pb they contain is relatively low compared to the Pb content of primary and secondary phases. This is likely due to adsorption and substitution reactions that act to dilute the Pb content of tertiary solid phases. The majority of Pb phases (64%) in this sample occurred "attached" to other phases (Table 4) which is characteristic of precipitation and adsorption reactions. Only 32% of Pb phases occurred as liberated grains and 4.5% exist as "included" within other phases.

3.2.3 Sample 939 (Lab. no. S001575)

Sample 939 was collected from the 10- to 12-inch depth interval from a Quaternary fan deposit and is described as dark brown soil with mixed rock fragments. Total Pb content is 554 mg/kg with a sample pH of 7.6, indicating slightly alkaline conditions. EMPA analysis of sample 939 is presented in Table 2 and graphically depicted in Figure 12.

While six Pb phases were detected in this sample, the bulk of the Pb phases (65%) and Pb mass (82%) is contained in the tertiary FePb silicate phase. Pb released by oxidation of primary and secondary phases have probably been adsorbed or substituted into the matrix of soil Fe silicates (see equation [8] in Table 3). The second most abundant phase is MnPb oxide (21%) which because of its low Pb content contributes only 5% of total Pb mass. The frequency of cerussite is relatively low (6.5%), but it contributes over 11% of the total Pb mass in the sample. Galena and anglesite are absent, suggesting complete dissolution of these phases in favor of cerussite formation (see equations [2], [3], and [4] in Table 3). This is consistent with the alkaline environment of this sample in which cerussite would be relatively stable (see equation [3] in Table 3). Other phases present in trace amounts include FePb oxide (4.6%), Pb(M)O (<1%), and Pb phosphate (<1%). Of the phases present, almost 79% occur as liberated grains and almost 17% occur attached to other grains.

3.2.4 Sample 940 (Lab no. S001576)

Sample 940 was collected from an animal burrow in a vacant lot at the 12-inch depth interval and is described as a dark brown soil with small mixed rock fragments derived from disturbed colluvium. Total lead by ICP is 1390 mg/kg, with a sample pH of 6.4. EMPA analysis of sample 940 is presented in Table 2 and graphically presented in Figure 13. Nine Pb phases were detected by EMPA with the majority consisting of tertiary oxide phases. Primary and secondary minerals (galena and cerussite) occurred in subordinate amounts and anglesite is completely absent. The tertiary phase with the greatest frequency of occurrence (44%) and relative Pb mass (50%) is MnPb oxide, suggesting coprecipitation or adsorption of Pb by Mn, similar to the reaction in equation (11) (Table 3), is occurring in this sample. FePb oxide was also frequently detected (30%) but represents only 16% of the total Pb mass. The remaining 34% of Pb mass is roughly distributed among FePb silicate (8.6%), galena (7%), Pb silicate (5%), Pb phosphate and cerussite (4.3%), and Pb(M)O and FePb sulfate (<3%). The majority of Pb phases (69%) occur as liberated grains, while almost 29% occur attached to other phases. Only 1.6% exist included within other phases.

3.2.5 Sample 943 (Lab no. S001579)

Sample 943 was collected from a depth of 6'-8' from the excavation of a new home within mixed undisturbed (?) Quaternary alluvium and is described as soil, sand, and mixed rock fragments. Total Pb in this sample (49,500 mg/kg) is the highest concentration of all the Rico samples. Sample pH is slightly alkaline at 7.2.

EMPA analysis of sample 943 is presented in Table 2 and illustrated in Figure 14. Five Pb phases were detected with the majority of phases being the primary and secondary minerals cerussite (frequency = 43%), anglesite (14%), and galena (15%). The apparently elevated Pb concentration (49,500 mg/kg) in this sample is more typical of the concentrations found in bedrock samples than those found in alluvium/colluvium samples, and is likely due to the high percentage of primary and secondary mineral phases. The predominant tertiary phase is FePb oxide (frequency = 22%). The second most frequent tertiary phase is FePb oxide (21%), but this phase contributes <2% of the Pb mass. This sample exhibits over 93% liberated grains, which is similar to that observed in the bedrock group of samples. Approximately 5.5% occurred included in other grains.

A photomicrograph of sample 943 is included as Figure 21, and illustrates the paragenetic relationship between a secondary Pb phase (PbCO_3) and a tertiary Pb phase (MnPb oxide) wherein the dissolution of PbCO_3 releases Pb^{+2} ions which are subsequently incorporated into the structure of the Mn oxide, either through adsorption or coprecipitation. The MnPb oxide has formed a precipitate encapsulating the PbCO_3 grains.

3.2.6 Sample 945 (Lab no. S001581)

Sample 945 was collected from the 36"-48" depth interval from the foundation excavation of a cabin in mixed undisturbed Quaternary colluvium; and is described as soil, silt, sand, with fragments of carbonates, latite porphyry, quartzite, and other rock types. Total lead by ICP is 1570 mg/kg, with a sample pH of 6.9.

EMPA analysis of sample 945 is presented in Table 2 and graphically presented in Figure 15. Five Pb phases were detected, consisting of two secondary Pb phases (cerussite and anglesite) and three tertiary phases (FePb silicate, MnPb oxide, and FePb oxide). Galena was absent in this sample suggesting complete dissolution of this phase in favor of formation of secondary and tertiary phases. The most abundant Pb phase is FePb silicate (frequency of occurrence = 84%) and which also contributes the majority of the Pb mass (71%). Coprecipitation of free Pb^{+2} (similar to the reaction in equation (8) in Table 3) may be the dominant pedogenic process operating in this sample. The remaining four phases represent subordinate Pb phases with respect to both frequency and total Pb mass (Figure 15). Of the Pb phases detected, approximately 83.3% occurred as liberated grains, and 16% occurring attached to other grains. None of the phases occurred included within other phases.

3.3 Grandview Smelter Sample 96-CH-01 (Lab no. S001919)

Sample 96-CH-01 is a 5-point composite sample collected from surface soil (0- to 2-inch depth interval) at the Grandview Smelter site. The sample is described as brown soil, with angular clastic rock, rock fragments, rounded gravel, slag and cinders. A rounded, massive pyrite pebble at least 1 inch in size was also observed (Table 1). Total Pb is 6290 mg/kg, with a pH of 7.4 indicating slightly alkaline conditions.

EMPA results for sample 96-CH-01 are presented in Table 2 and graphically presented in Figures 4 and 16. Results indicate that while slag (an anthropogenic phase) is the most abundant Pb phase present in this sample (frequency of occurrence = 94%), it accounts for only 3.6% of the total Pb mass. The bulk of Pb mass is contained within the tertiary oxide (PbO - 48%) and secondary sulfate (anglesite - 41%) phases. These phases are present in sparse amounts, and account for only 1.5% and 2.7% of Pb phase frequency, respectively. The remaining 7% of sample Pb mass is distributed among four minor phases consisting of galena (6%), FePb sulfates (<1%), MnPb oxides (0.5%), and FePb oxides (0.2%). Because slag is the dominant Pb phase, almost two-thirds (64%) of the Pb phases are "included" (i.e., contained within other phases) and only 36% exist as liberated phases. Because "included" Pb phases are contained within other solids, there is limited surface area available for reaction by soil solutions and oxygen, thereby greatly reducing the potential for dissolution and subsequent release of Pb. Slag Pb tends to be relatively stable as a result.

3.4 Roadfill Samples

Two samples of roadfill (96-CH-02 and 96-CH-04) were submitted for EMPA analysis. The combined frequency of occurrence of Pb phases for these samples is depicted on Figure 5. A total of eleven Pb-bearing phases were detected in these samples, including particles of paint and slag (Figure 5). While the dominant Pb phase in the roadfill samples is a tertiary phase (FePb oxide), there appears to be a relatively equal mix of primary, secondary, and tertiary phases in these samples. This may be due to a waste-rock source of these samples, a material commonly used for road building in mining districts. Both samples exhibit high proportions of FePb oxides, slag material, and galena. The galena in these samples contributes the bulk of the relative Pb mass, with little Pb mass being present in the tertiary and anthropogenic phases.

3.4.1 Sample 96-CH-02 (Lab no. S001920)

Sample 96-CH-02 represents a 4-point composite and was collected from the 0- to 2-inch depth interval from a graded berm approximately 5 feet south of a road and is composed of varied lithology of gravel size (Table 1). Total Pb in this sample is 2260 mg/kg, with a pH of 7.8. This pH indicates a solidly alkaline environment at this location. High pH's in soil

and rock are the result of abundant carbonate minerals present in the Rico area (McKnight 1974).

EMPA analysis of sample 96-CH-02 are presented in Table 2 and graphically presented in Figure 17. EMPA results indicate that eleven Pb phases were detected in this sample, with several primary (galena), secondary (cerussite), and tertiary (FePb oxide and FePb silicate) phases present in similar proportions (Figure 17). The most abundant Pb phase (slag) was counted at a frequency of 26.5% but contributes less than 1% of the total Pb mass (Table 2). Galena is the primary Pb-bearing mineral, contributing over 80% of total Pb mass even though the frequency of occurrence is 22.6%. The tertiary phase FePb silicate was detected at a frequency of 22.5%, while contributing only 4.5% of Pb mass. FePb oxide, MnPb oxide, and cerussite contribute similar percentages of Pb mass. Other compounds such as anglesite, paint, Pb(M)O, Pb phosphate, and FePb sulfate are relatively insignificant contributors to the total Pb mass. FePb sulfate (plumbojarosite) is prevented from forming in any significant amounts in this sample due to the high pH conditions (plumbojarosite formation favors low pH as shown in equation (12) in Table 3) and apparent lack of sulfate. This is supported by the paucity of PbSO₄ in this sample as well. Of the 11 phases detected, approximately 45.3% occurred as liberated phases with an equivalent amount (42.6%) existing included within other phases.

A photomicrograph of sample 96-CH-02 is illustrated in Figure 22. The photomicrograph depicts a large grain of ferric oxyhydroxide (goethite?) that is host to several primary sulfide phases including galena (PbS) and sphalerite (ZnS), as well as quartz (SiO₂). Several sulfide phases (bright white regions) are observed to be encapsulated within the FeOOH matrix protecting them from alteration and dissolution by oxidizing soil solutions. Dissolution of exposed FeOOH and quartz releases Fe and H₄SiO₄, respectively, to the soil solution which are then able to complex with Pb⁺² to form FePb silicates, according to a reaction similar to equation (8) (Table 3). Lead is also scavenged by Fe- and Mn- oxides to form FePb oxide and MnPb oxide (Table 3 and Figure 17).

3.4.2 Sample 96-CH-04 (Lab no. S001922)

Sample 96-CH-04 is a 5-point composite sample collected from the 0- to 2-inch depth interval from Silver Street and is described as muddy, with 1/2" and smaller angular varied lithology (Table 1). Total Pb concentration measured by ICP is 2300 mg/kg. The sample pH (7.9) is alkaline probably due to the presence of locally-derived carbonate minerals.

EMPA results for 96-CH-04 are presented in Table 2 and depicted in Figure 19. Results indicate that nine Pb phases were detected, with an apparently equal mix of primary (galena), secondary (cerussite), and tertiary (MnPb oxide and FePb oxide) Pb phases. Anthropogenic phases (slag and Pb(M)O) are also present but in relatively minor amounts. The most abundant Pb phases are FePb oxide (frequency = 31.4%) and MnPb oxide (25%); however, these phases contribute only 4.6% and 8%, respectively, of total Pb mass. In contrast, galena has a frequency of 19.8%, but contributes over 58% of the total Pb mass, illustrating the diluting effect observed as Pb is cycled from primary and secondary phases to tertiary phases. Similarly, cerussite has a frequency of only 12%, but contributes almost 28% of Pb mass. While slag has a frequency of over 8%, the contribution to total Pb mass is negligible (<0.04%). The contribution to total Pb mass and frequency of occurrence of the remaining phases (FePb silicate, Pb(M)O, Pb phosphate, and FePb sulfate) are relatively insignificant (Table 2). Of the phases detected, the majority (53.4%) occur as liberated grains; 26.1% occur as attached; 11.9% occur included in other phases; and 8.5% occur as rims (Table 4). The distribution of physical associations observed is probably related to the large number of different Pb phases detected in this sample. Similar distributions are also observed in Sample 96-CH-02 (Table 4).

3.5 Van Winkle Mine Sample (Lab no. S001921)

Sample 96-CH-03, collected from the VanWinkle mine site, is a 3-point composite sample collected from the 0- to 2-inch depth interval from a bare steep slope, and is described as muddy, with a varied lithology, with some visible pyrite (Table 1). Total Pb concentration is 8770 mg/kg, with a sample pH of 8.2. This is the highest pH measured in the Rico samples and is probably due to the presence of carbonate minerals such as cerussite (PbCO_3).

EMPA results are presented in Table 2 and depicted graphically in Figures 6 and 18. EMPA results indicate that this sample is dominated by MnPb oxide in terms of frequency (35%), but the bulk of the Pb mass is due to the presence of galena (41.7%) and cerussite (42%). MnPb oxide contributes only 9% of total Pb mass. Another tertiary phase, FePb oxide, has a frequency of 21%, yet contributes only 2.5% of Pb mass. Anglesite has a frequency of 3%, and contributes 4.5% of Pb mass. The contribution of FePb oxide to the frequency and mass is relatively insignificant. As shown on Table 4, the physical associations of Pb phases are roughly equal between liberated phases (32.7%) and rimmed phases (37.8%), with lesser numbers existing as attached (15.3%) and included (14.2%).

A photomicrograph of sample 96-CH-03 is presented in Figure 20. This figure illustrates the paragenetic relationship between the primary Pb phase galena (PbS) and the secondary Pb phases anglesite (PbSO_4) and cerussite (PbCO_3). Anglesite occurs as an oxidation layer surrounding the galena core, and probably formed according to reaction (1) in Table 3. However, due to the high pH of this sample, anglesite converted to cerussite in the presence of high dissolved bicarbonate as represented by equation (4) in Table 3. The formation of a rim of cerussite around the anglesite has protected the anglesite from further alteration allowing the three chemically dissimilar Pb phases to co-exist.

4.0 Conclusions

EMPA analysis of Rico samples has established the presence of numerous Pb solids of varying composition consisting of primary, secondary, tertiary, and anthropogenic Pb phases. Primary Pb phases consist solely of galena (PbS); whereas secondary Pb phases consist of anglesite (PbSO_4) and cerussite (PbCO_3). Tertiary phases consist of a suite of Pb-bearing oxide, silicate, phosphate, organic, and sulfate phases. The tertiary oxides are Fe- and Mn-rich whereas the Pb-bearing silicates are dominated by Fe. Pb organics represent soil organic matter that contains adsorbed Pb that was released by alteration of primary, secondary, and tertiary phases. The phosphates and sulfates are minor components of the Rico samples. Anthropogenic phases detected consist of slag, paint, solder, and mixed Pb-metal oxides (Pb(M)O).

Primary and secondary phases are typically abundant in Rico bedrock outcrop samples and in some samples of alluvium, colluvium, and the Van Winkle mine site sample. In general, the proportion of primary and secondary Pb phases decrease in alluvium and colluvium as oxidation and alteration weathering processes alter these phases to more stable Pb tertiary phases. Tertiary phases are almost completely absent from the bedrock samples. Anthropogenic phases are abundant in the Grandview Smelter site sample and occur in minor amounts in some alluvium and colluvium samples. In general, while some anthropogenic phases are abundant, they typically contain very little Pb. The mass of Pb contained in the various Pb phases is greatest in the primary and secondary phases and decreases significantly in the tertiary and anthropogenic phases. Except for the presence of some anthropogenic Pb phases in a few samples, the majority of Pb phases observed in the Rico samples appear to represent the natural sequence of Pb geochemical cycling as primary Pb phases are altered to secondary and tertiary forms.

References

Black, C.A. (1965) *Methods for Soil Analysis. Part 2. Chemical and Microbiological Properties*. Black, C.A., Ed.; American Society of Agronomy, Inc.: Madison, WI, pp. 914.

Davis, A., Drexler, J.W., Ruby, M.V., and Nicholson, A. (1993) Micromineralogy of Mine Wastes in Relation to Lead Bioavailability, Butte, Montana. *Environ. Sci. Technol.* 27, 1415-1425.

Drexler, J. (1996) Personnel communication.

Link, T.E., Ruby, M.V., Davis, A., and Nicholson, A.D. (1994) Soil Lead Mineralogy by Microprobe: An Interlaboratory Comparison. *Environ. Sci. Technol.* 28, 985-988.

McKnight, E.T. (1974) *Geology and Ore Deposits of the Rico District, Colorado*. Geological Survey Professional Paper 723, U.S. Government Printing Office, Washington: 1974.

Tables

Table 1. Field Lithologic Descriptions of Rico Samples. *

Sample	Description
906	Hornblende Latite Porphyry. 8 foot chip sample across outcrop in road cut. TKhlp is dark greenish-gray, strongly chloritized, with N78°W striking quartz-hematite-pyrite-galena veinlets up to 1 inch thick. Some veinlets are vuggy, with comb quartz, pyrite, hematite, galena, iron oxides (limonite) and trace CuO staining.
910	Hornblende Latite Porphyry. 6 foot chip sample across outcrop. TKhlp is dark green, chloritized, brecciated; with limonite, MnO, and CuO on fractures and in breccia matrix. Some clay altered clasts.
917	Leadville Limestone. 6 foot chip sample across outcrop at caved Shamrock adit portal. Limestone is strongly chloritized, vuggy, contains pods and blebs of pyrite-sphalcritic-galena.
932	Mixed colluvium. Disturbed. Sample from utility right-of-way in front of log cabin. Sample is dark brown soil and mixed rock fragments. Sample depth is 3 to 6 inches.
938	Quaternary Fan Deposit - Undisturbed (Qf). Sample depth: 24 to 36 inches. Sample taken from utility excavation in undisturbed material. Sample material is unconsolidated, stratified, sand, silt, clay and gravel of mixed composition. Sample exhibited graded bedding.
939	Quaternary Fan Deposit - Undisturbed (?). Sample is dark brown soil with mixed rock fragments. Sample depth is 10 to 12 inches.
940	Mixed Colluvium - Disturbed (Qcol). Dark brown soil and small mixed rock fragments from animal burrow in vacant lot. Est. sample depth < 1 foot.
943	Mixed Quaternary Colluvium - Undisturbed (Qcol). Sample 943 was collected from a new home excavation at a depth of 6 to 8 feet. Sample is composed of soil, sand, and mixed rock fragments including: igneous porphyry, quartzite, sandstone, carbonate, and a few mineralized fragments. The mineralized fragments are sub-rounded, brown to black clasts or iron oxides and sulfides. One clast was CuO stained.
945	Mixed Quaternary Colluvium - Undisturbed (Qcol). Sample from depth of 36 to 48 inches in foundation excavation of log cabin. Sample is composed of soil, silt, sand, and angular to sub-rounded fragments of carbonates, latite porphyry, quartzite and other rock types. Matrix is tan to brown, limonitic.
96-CH-01	Grand View smelter site; duplicate sample RSS 08. Collected from under 2-3 feet of snow. Five point composite, 0-2 inches, frozen brown soil with angular clastic, rock fragments, rounded gravel, slag and cinders. Included at least one 1 inch across, rounded massive pyrite pebble.
96-CH-02	Road fill; duplicate sample RSS 29, 4-point composite, 0-2 inches, angular to subrounded gravel size. Varied lithology - from graded berm 5 feet south of the road and from road.
96-CH-03	Van Winkle Mine Site, duplicate sample RSS 32. 3-point composite, 0-2 inches, from bare steep south-facing slopes on west side of headframe. Muddy, varied lithology, less than 1 inch across material. Some with visible pyrite.
96-CH-04	Road fill sample. Does not duplicate previous sampling. 5-point composite, 0-2 inches, one-half inch and smaller, angular varied lithology, muddy. From Silver Street between bridge over Silver Creek and intersection with Mantz Avenue.

* Sample descriptions provided by Titan Environmental.

Sample Number	Sample Type	Primary	Secondary		Tertiary							Anthropogenic				Occurrence
		Galena	Anglesite	Cerussite	FePb Oxide	MnPb Oxide	Pb Phosphate	FePb Silicate	FePb Sulfate	Pb Organics	Pb Silicate	Pb(M)O	Slag	Solder	Paint	
908	Bedrock	42.1	37.9	7.6	10.9	0.4	0.4	*	*	*	*	*	*	*	*	Dominated by galena and anglesite
910	Bedrock	0.9	8	61	6	3.3	0.75	*	*	*	*	*	*	*	*	PbCO ₃ is dominant Pb phase
917	Bedrock	18.4	21.9	48.4	10.2	0.99	*	*	*	*	*	*	*	*	*	Cerussite and anglesite rich
932	Colluvium	0.13	*	*	32.2	18.1	*	24.8	*	6.2	*	7.6	7.2	1	*	Fe and Mn oxides dominant, lesser FePb silicates
938	Alluvium	1.1	0.3	7.7	41.6	26.3	15.7	*	*	*	6.4	*	*	0.66	*	Fe and Mn oxides dominant
939	Alluvium	*	*	6.5	4.7	21.3	1.4	65.2	*	*	*	0.85	*	*	*	FePb silicates are main Pb phase
940	Colluvium	0.6	*	0.5	28.9	43.8	2.7	14.1	6.7	*	0.87	0.7	*	*	*	Tertiary phases dominant, esp. oxides
943	Colluvium	15.1	13.6	42.9	21.5	*	*	6.7	*	*	*	*	*	*	*	Cerussite and FePb oxides
945	Colluvium	*	0.4	0.9	8.6	6.1	*	64	*	*	*	*	*	*	*	Dominated by FePb silicates
96-CH-01	Grand View	0.3	2.7	*	0.2	0.2	*	*	0.8	*	*	*	94	*	*	Slag
96-CH-02	Roadfill	22.6	0.2	3.2	16.4	5.8	0.5	22.6	1.2	*	*	0.7	26.5	*	0.5	Equal mix of primary, secondary, tertiary, anthropogenic
96-CH-03	Van Winkle	17.5	2.9	22.5	21.2	35.1	*	0.8	*	*	*	*	*	*	*	Mix of primary, secondary, and tertiary phases
96-CH-04	Roadfill	19.8	*	12	31.4	25.2	1.1	1.2	0.8	*	*	0.1	8.4	*	*	Dominated by tertiary oxides, with lesser primary/secondary

* Not detected

Table 2. Frequency of Occurrence of Pb Phases in Rico Samples

	Reaction	Explanation
(1).	$\text{PbS} + 2\text{O}_2 = \text{PbSO}_4$	Direct oxidation of galena to anglesite by oxygen.
(2).	$\text{PbS} = \text{Pb}^{+2} + \text{S}^{-2}$	Dissociation of galena releasing Pb^{+2} ion to surrounding soil solution.
(3).	$\text{Pb}^{+2} + \text{HCO}_3^- = \text{PbCO}_3 + \text{H}^+$	Formation of cerussite from Pb^{+2} ion and bicarbonate.
(4).	$\text{PbSO}_4 + \text{HCO}_3^- = \text{PbCO}_3 + \text{SO}_4^{-2} + \text{H}^+$	Equilibrium between anglesite and cerussite at near-neutral pH.
(5).	$\text{FeS}_2 + 7/2\text{O}_2 + \text{H}_2\text{O} = \text{Fe}^{+2} + 2\text{SO}_4^{-2} + 2\text{H}^+$	Oxidation of pyrite with release of ferrous ion and acidity to solution.
(6).	$\text{Fe}^{+3} + 3/2\text{Pb}^{+2} + 3\text{H}_2\text{O} = (\text{Fe,Pb}_{1.5})_2\text{O}_3 + 6\text{H}^+$	Coprecipitation of Pb^{+2} with Fe^{+3} to form mixed FePb oxide.
(7).	$\text{Fe}^{+3} + 3/2\text{Pb}^{+2} + 3\text{H}_2\text{O} = (\text{Fe,Pb}_{1.5})(\text{OH})_3 + 3\text{H}^+$	Coprecipitation of Pb+2 with Fe+3 to form mixed hydroxide.
(8).	$\text{Fe}^{+2} + \text{Pb}^{+2} + \text{H}_4\text{SiO}_4 = (\text{Fe,Pb})\text{SiO}_3 + 2\text{H}^+ + \text{H}_2\text{O}$	Coprecipitation of Pb+2 with Fe+2 to form FePb silicates.
(9).	$\text{MnCO}_3 + \text{H}^+ = \text{Mn}^{+2} + \text{HCO}_3^-$	Dissolution of rhodochrosite to yield dissolved Mn^{+2} .
(10).	$\text{MnSiO}_3 + 2\text{H}^+ + \text{H}_2\text{O} = \text{Mn}^{+2} + \text{H}_4\text{SiO}_4$	Dissolution of rhodonite to yield dissolved Mn^{+2} and silica.
(11).	$\text{Mn}^{+4} + \text{XPb}^{+2} + 2\text{H}_2\text{O} = (\text{Mn,Pb}_x)\text{O}_2 + 4\text{H}^+$	Coprecipitation of Pb+2 with Mn+4 to form MnPb oxides.
(12).	$\text{Pb}^{+2} + 6\text{Fe}^{+3} + 4\text{SO}_4^{-2} + 12\text{H}_2\text{O} =$ $\text{PbFe}_6(\text{SO}_4)_4(\text{OH})_{12} + 12\text{H}^+$	Formation of FePb sulfate mineral "plumbojarosite".
(13).	$\text{Pb}^{+2} + \text{organic} = \text{Pb-organic}$	Adsorption of Pb^{+2} ion by organic matter to form Pb organics.

Table 3. Some Proposed Mineral Reactions Controlling Observed Pb Phases in Rico Samples.

**Table 4. Summary Data of Physical Associations of
Pb Phases in Rico Samples**

Field Sample	% Liberated	% Attached	% Included	% Rimmed
906	95.8%	3.1%	0.3%	0.8%
910	83.8%	9.0%	5.7%	1.5%
917	95.5%	1.9%	1.1%	1.5%
932	67.3%	29.9%	1.9%	0.9%
938	31.8%	63.6%	4.5%	0.0%
939	78.7%	16.7%	0.0%	4.6%
940	69.1%	28.5%	1.6%	0.8%
943	93.3%	1.2%	5.5%	0.0%
945	83.3%	16.0%	0.0%	0.8%
96-CH-01	36.3%	0.0%	63.7%	0.0%
96-CH-02	45.3%	10.0%	42.6%	2.1%
96-CH-03	32.7%	15.3%	14.2%	37.8%
96-CH-04	53.4%	26.1%	11.9%	8.5%

Figures

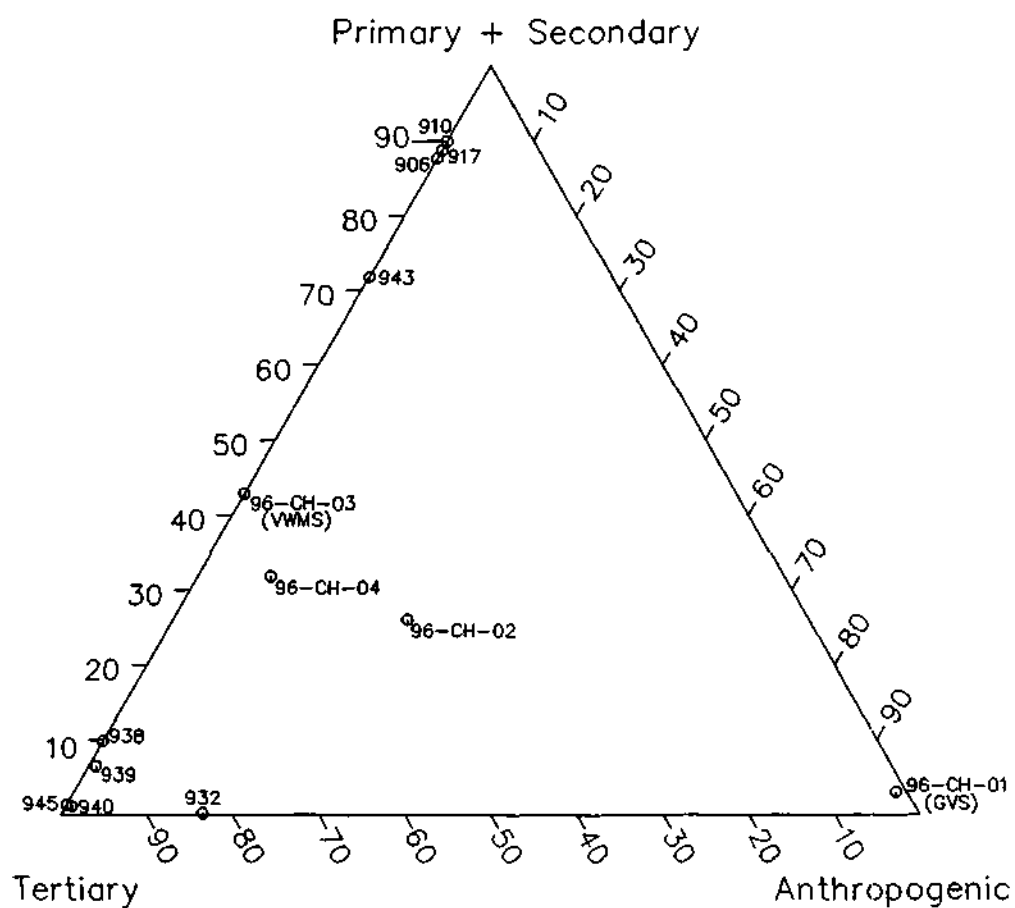


Figure 1. Ternary diagram showing relationship between Primary + Secondary, Tertiary, and Anthropogenic Pb phases in Rico Samples based on frequency of occurrence presented in Table 2.

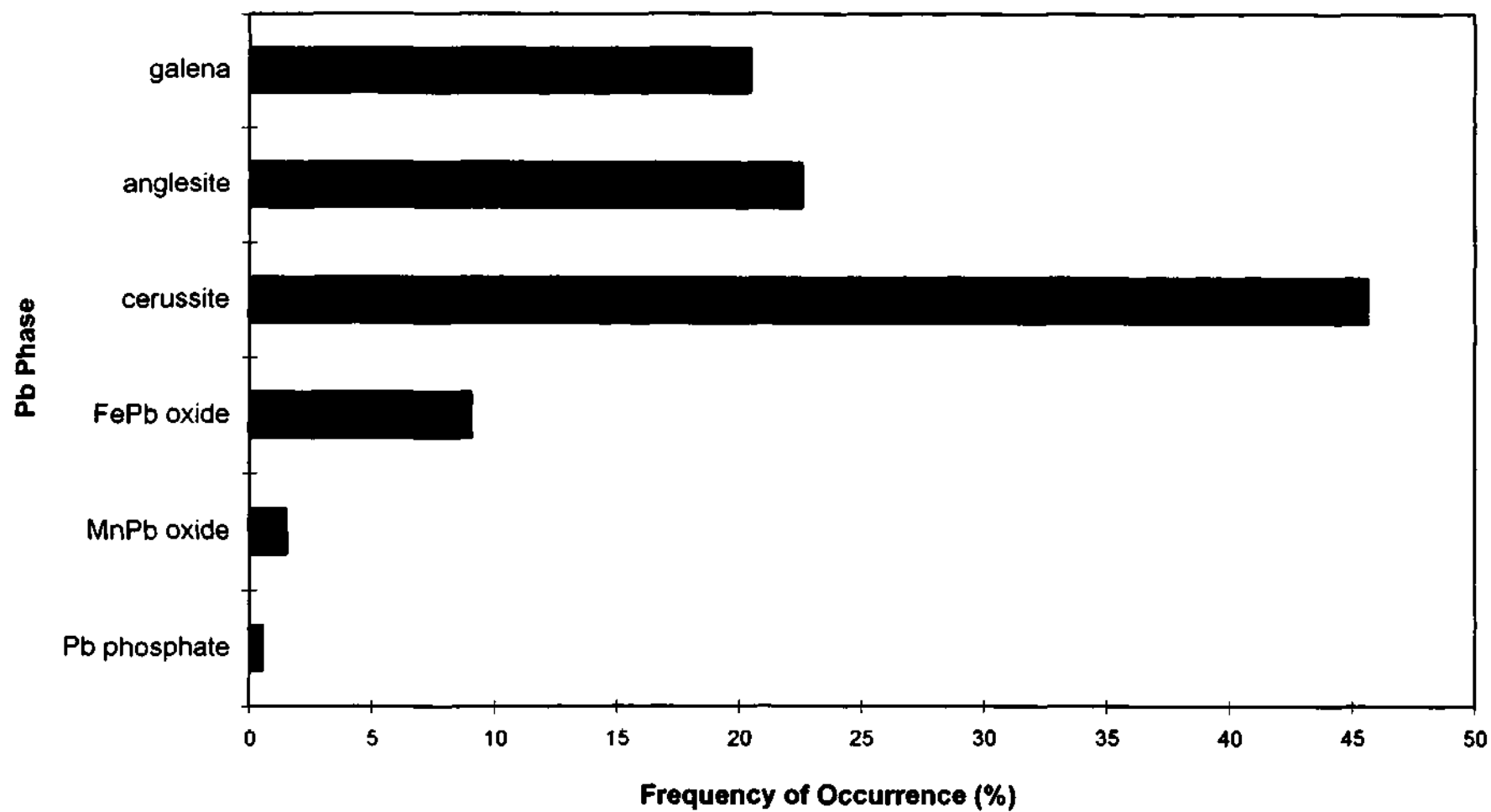


Figure 2. Frequency of Pb phases occurring in Rico bedrock samples.

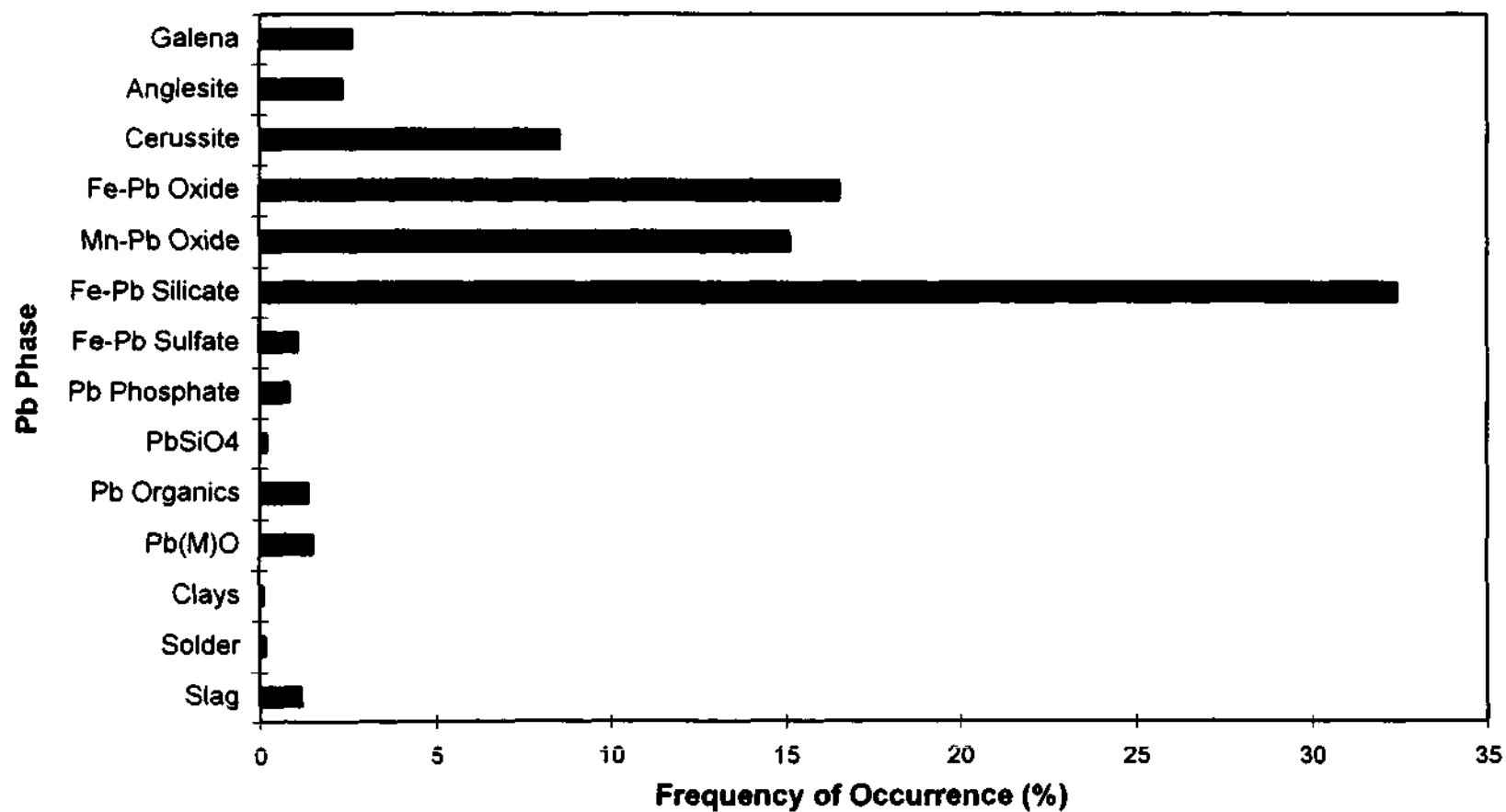


Figure 3. Frequency of Pb phases in alluvium/colluvium samples.

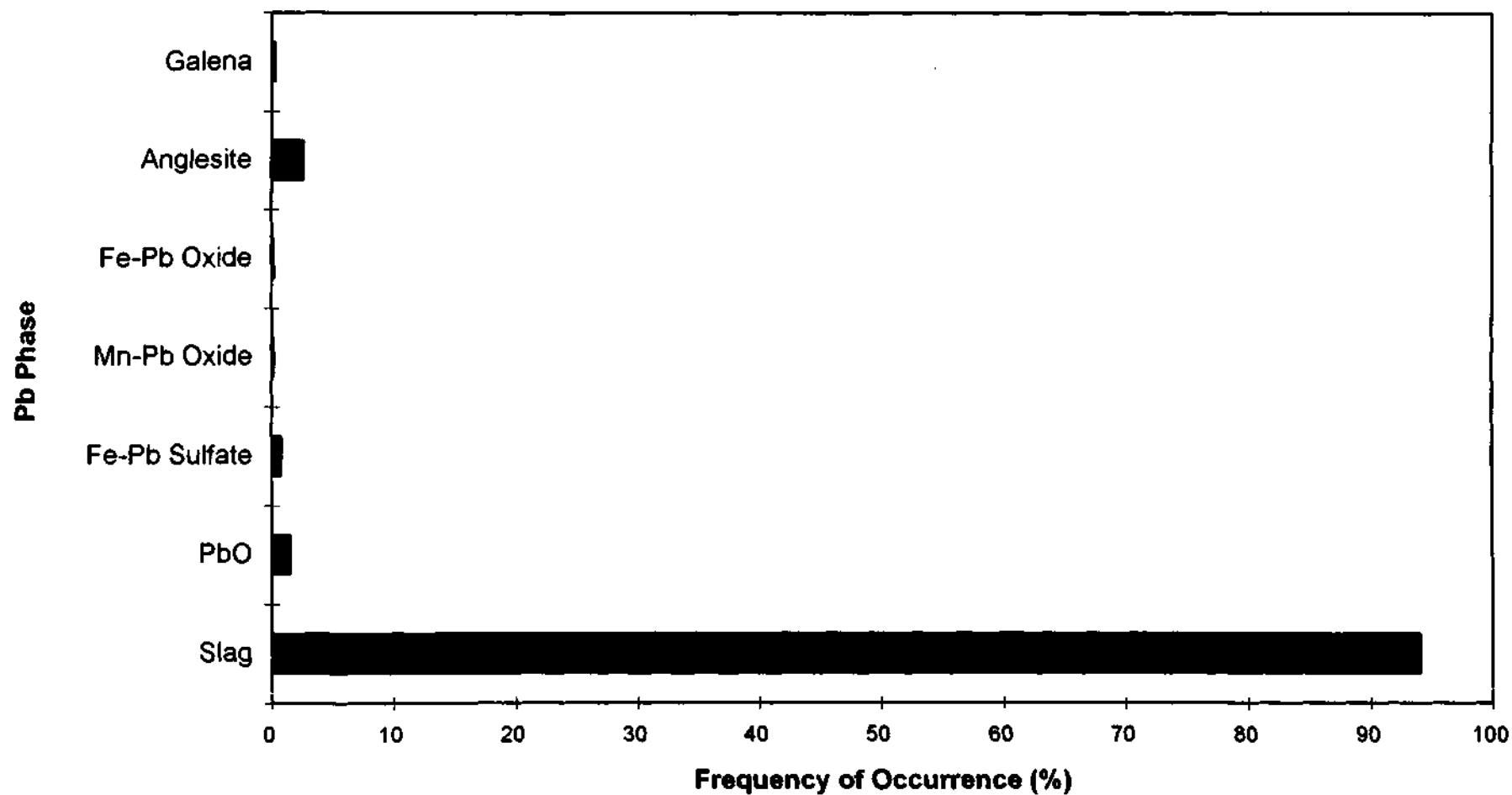


Figure 4. Frequency of Pb phases occurring in Grandview Smelter sample.

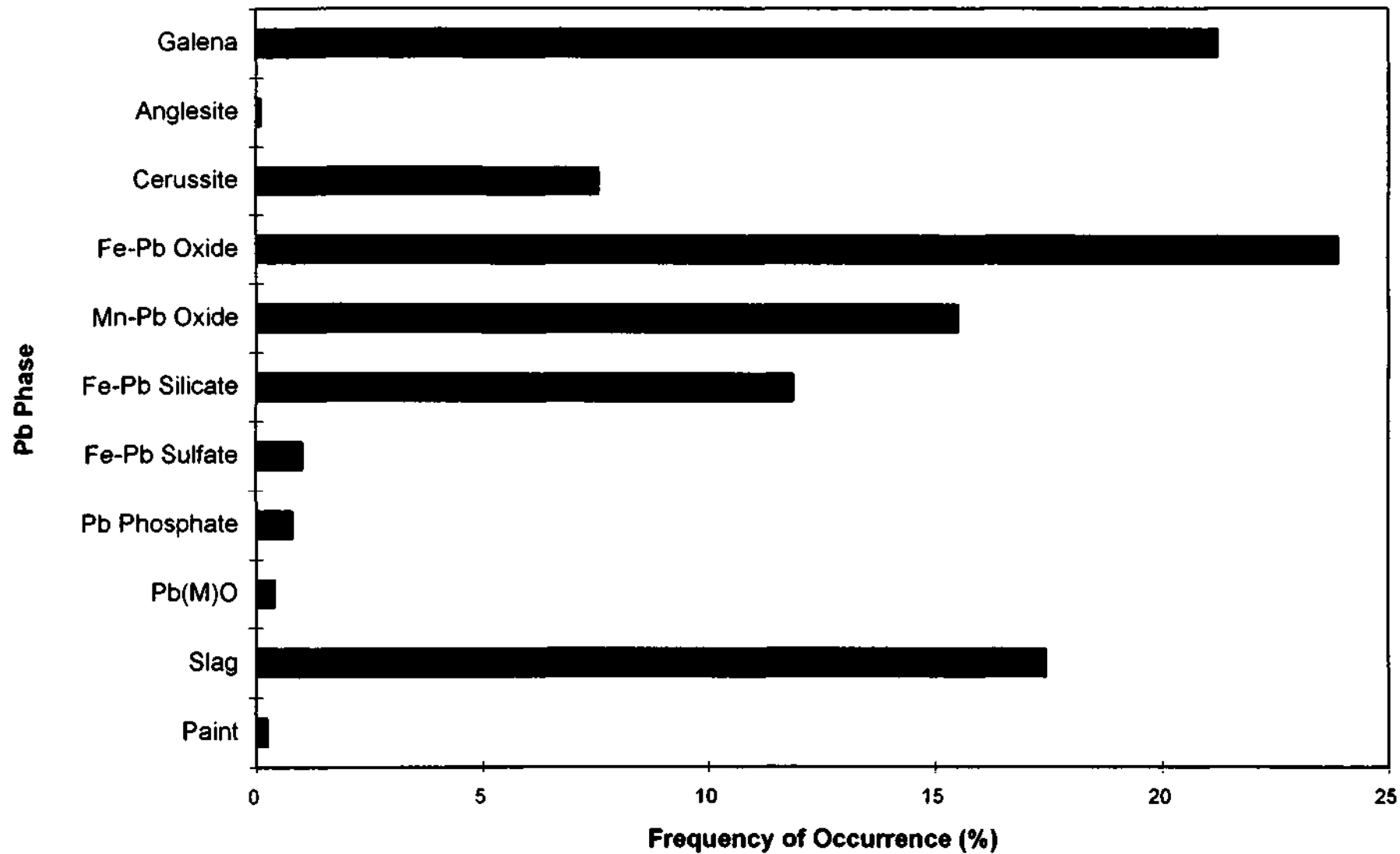


Figure 5. Frequency of Pb phases occurring in roadfill samples.

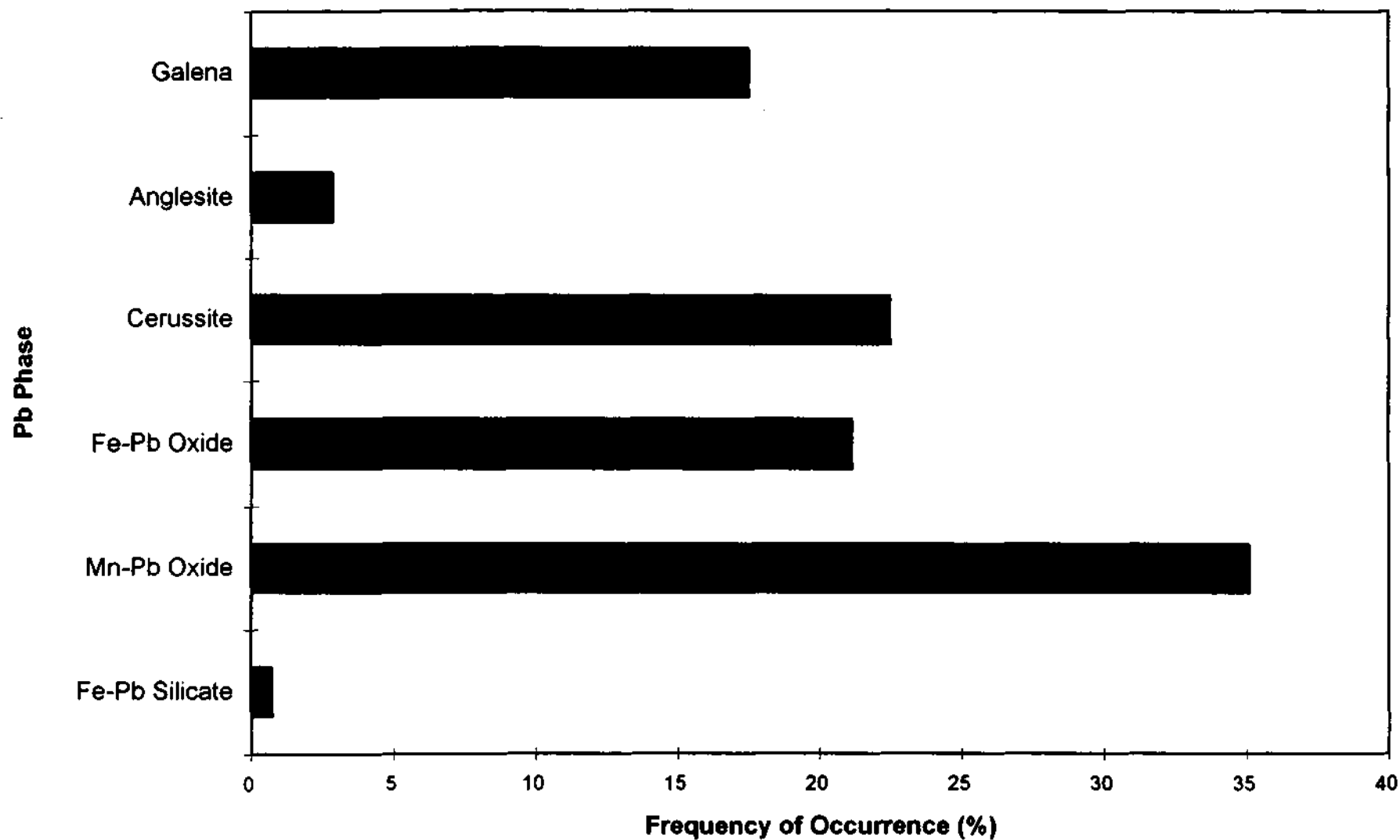


Figure 6. Frequency of Pb phases occurring in Van Winkle mine sample.

Rico, Colorado

Lab Sample SOO1542
(Field Sample #906)

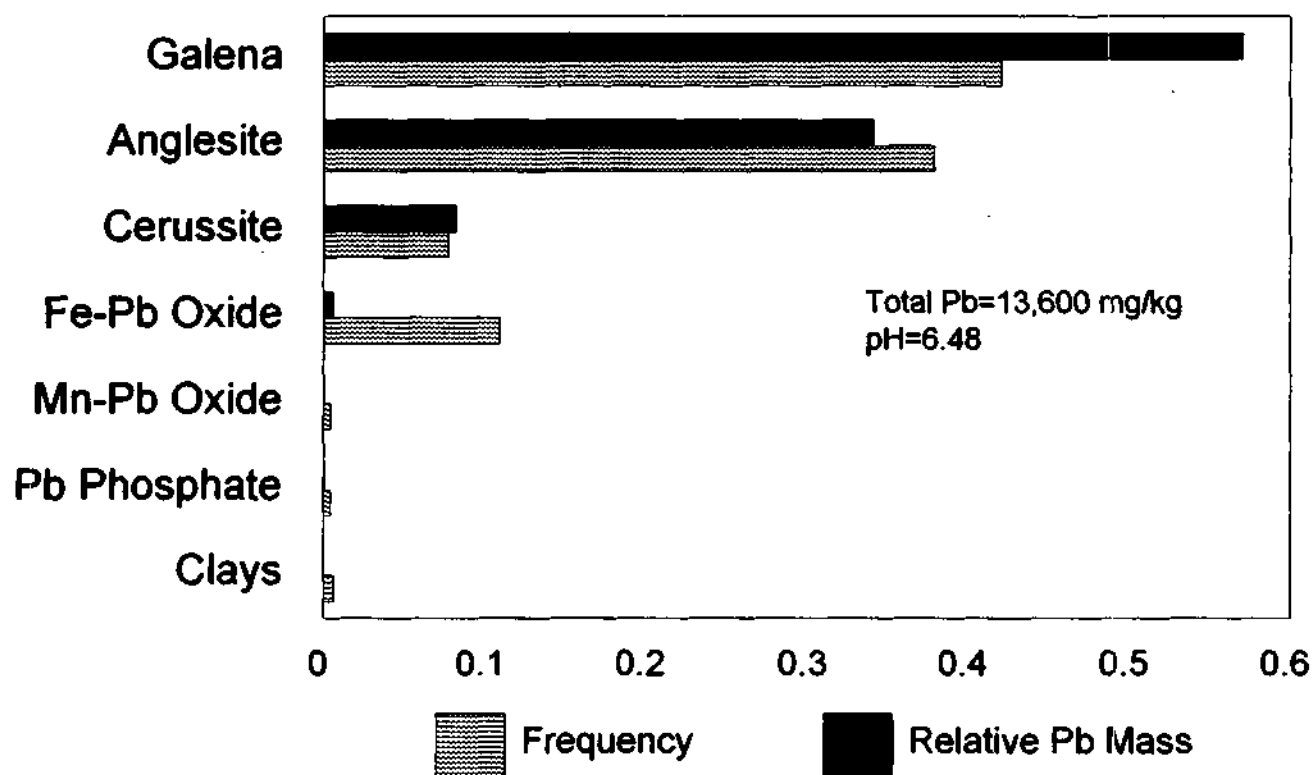


Figure 7. Frequency and Relative Pb Mass of Pb Phases in Bedrock Hornblende Latite Porphyry.

Rico, Colorado

Lab Sample SOO1546

(Field Sample #910)

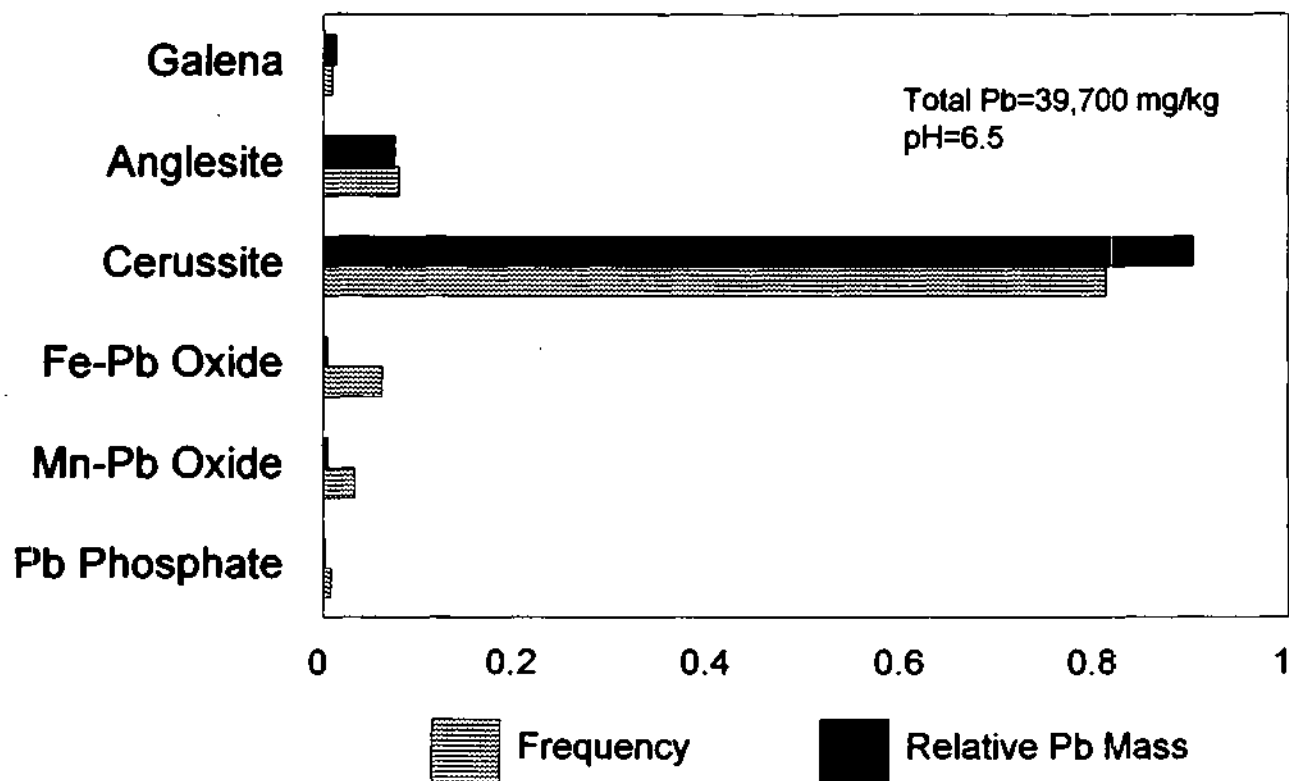


Figure 8. Frequency and Relative Pb Mass of Pb Phases in Bedrock Hornblende Latite Porphyry.

Rico, Colorado

Lab Sample SOO1553

(Field Sample #917)

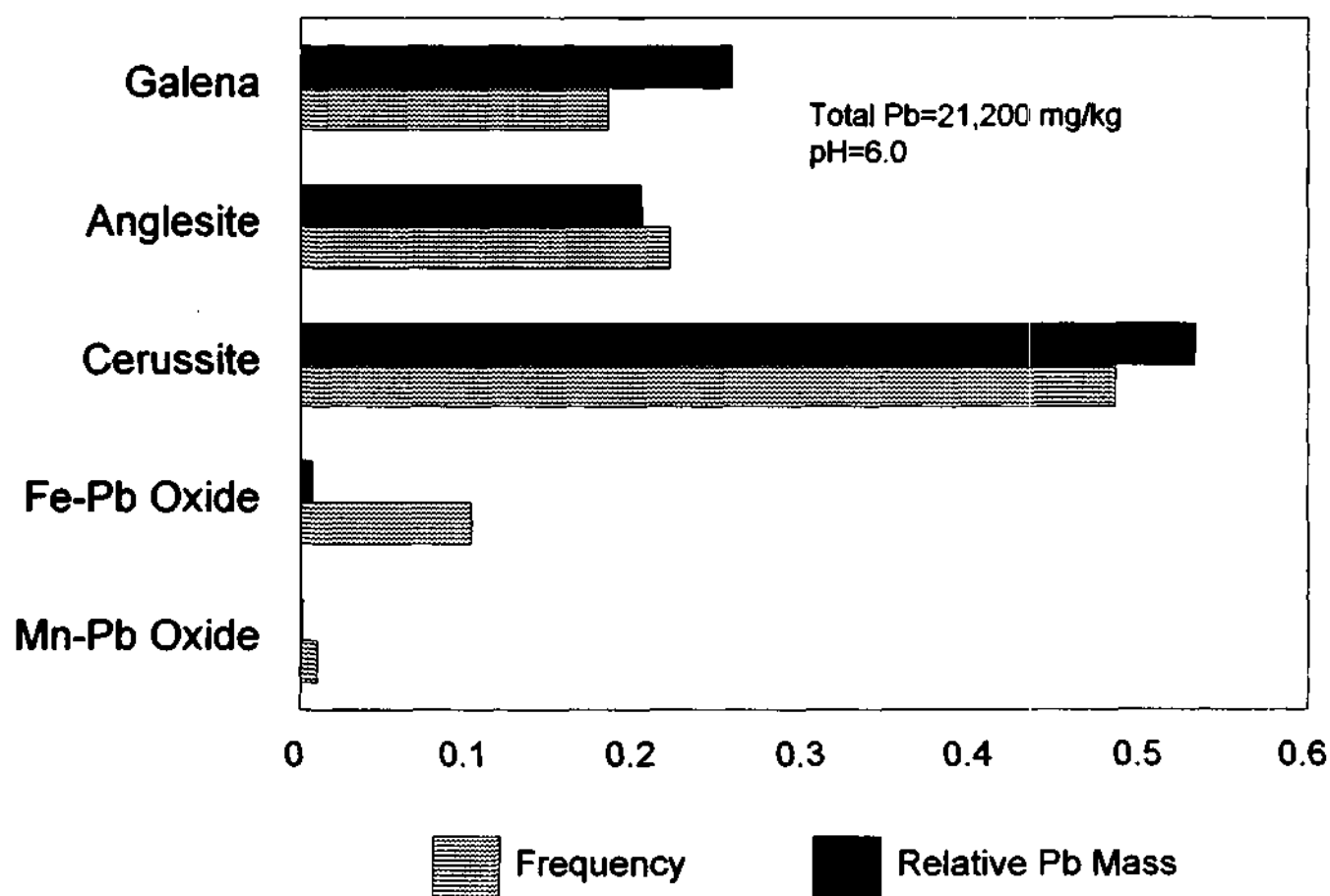


Figure 9. Frequency and Relative Pb Mass of Pb Phases in Bedrock Leadville Limestone.

Rico, Colorado

Lab Sample SOO1568

(Field Sample #932)

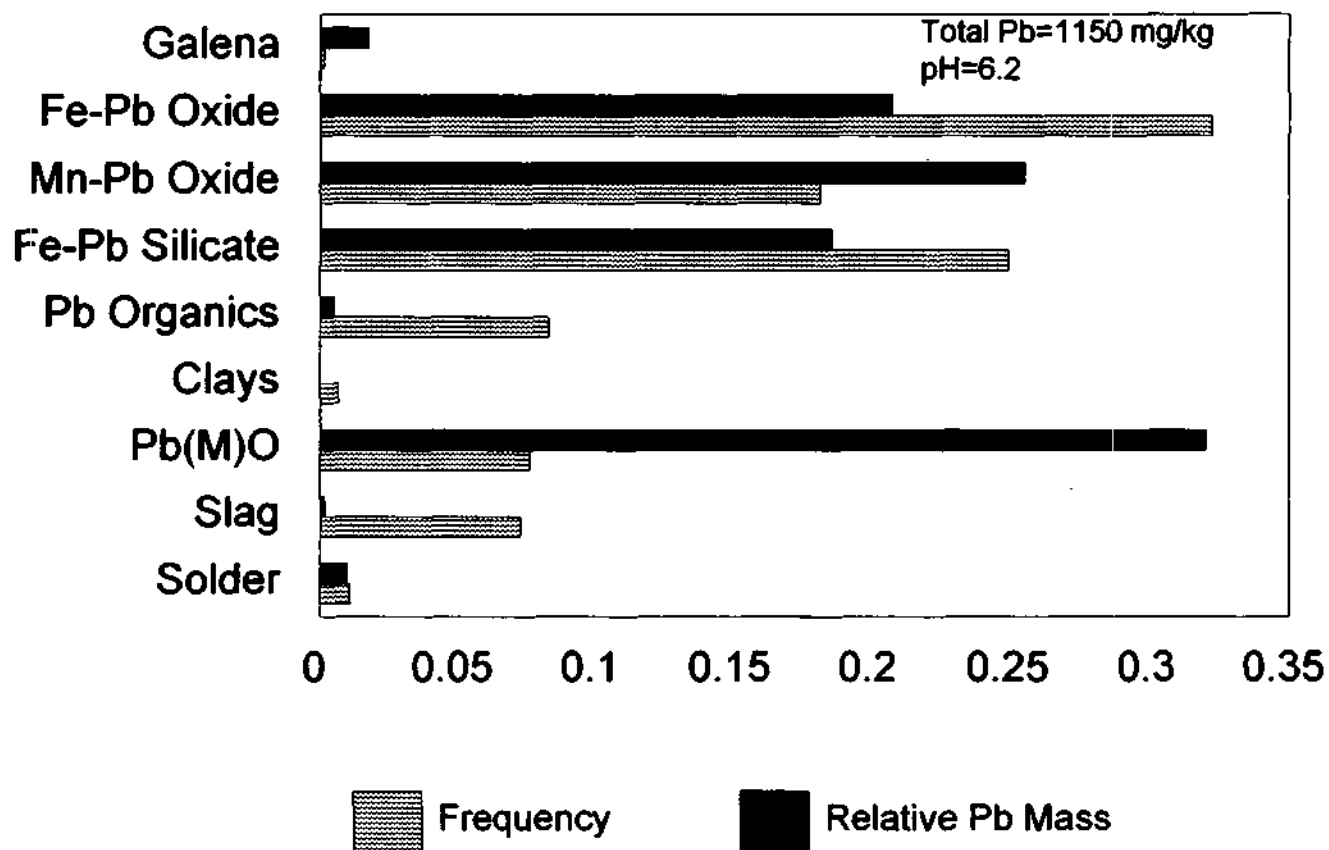


Figure 10. Frequency and Relative Pb Mass of Pb Phases in Disturbed Colluvium.

Rico, Colorado

Lab Sample SOO1574

(Field Sample #938)

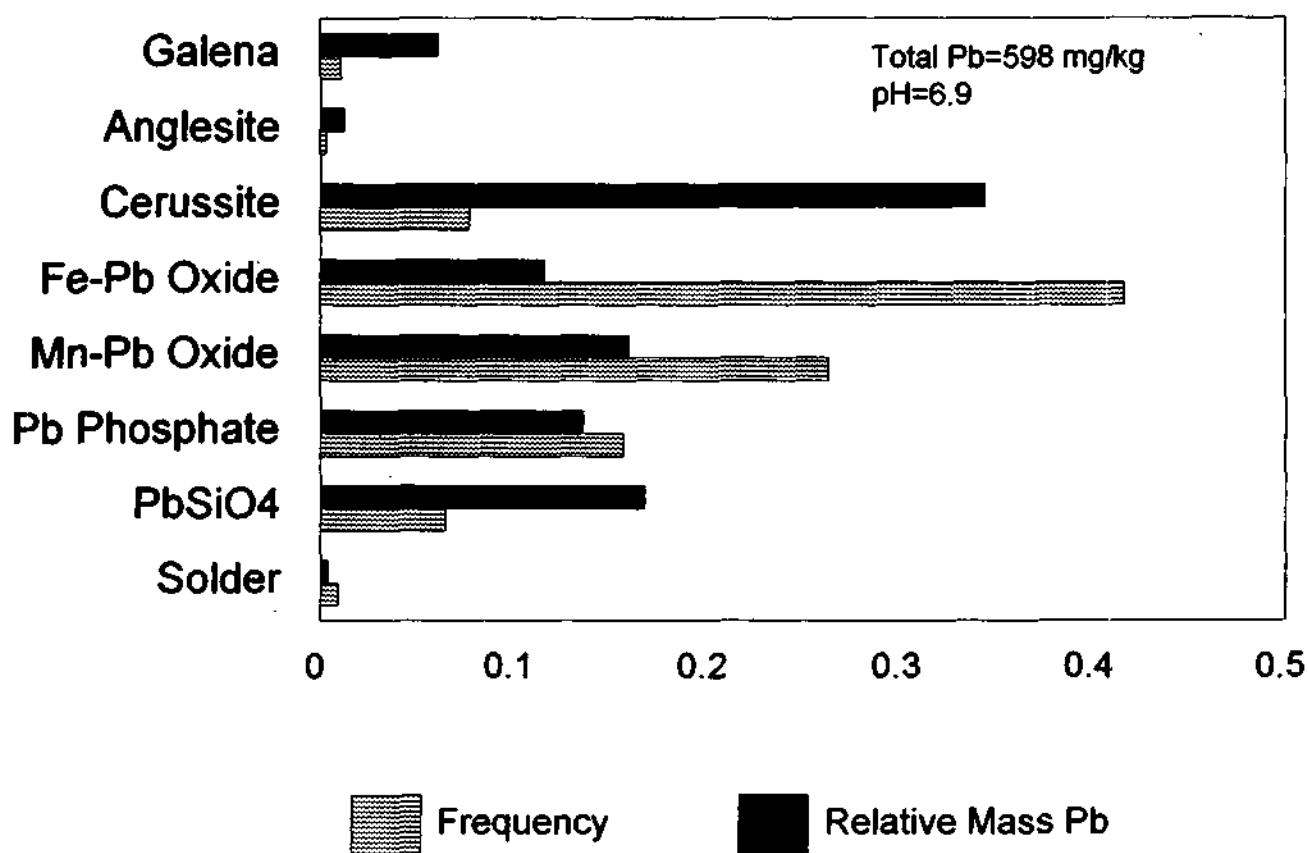


Figure 11. Frequency and Relative Pb Mass of Pb Phases in Undisturbed Alluvium.

Rico, Colorado

Lab Sample SOO1575
(Field Sample #939)

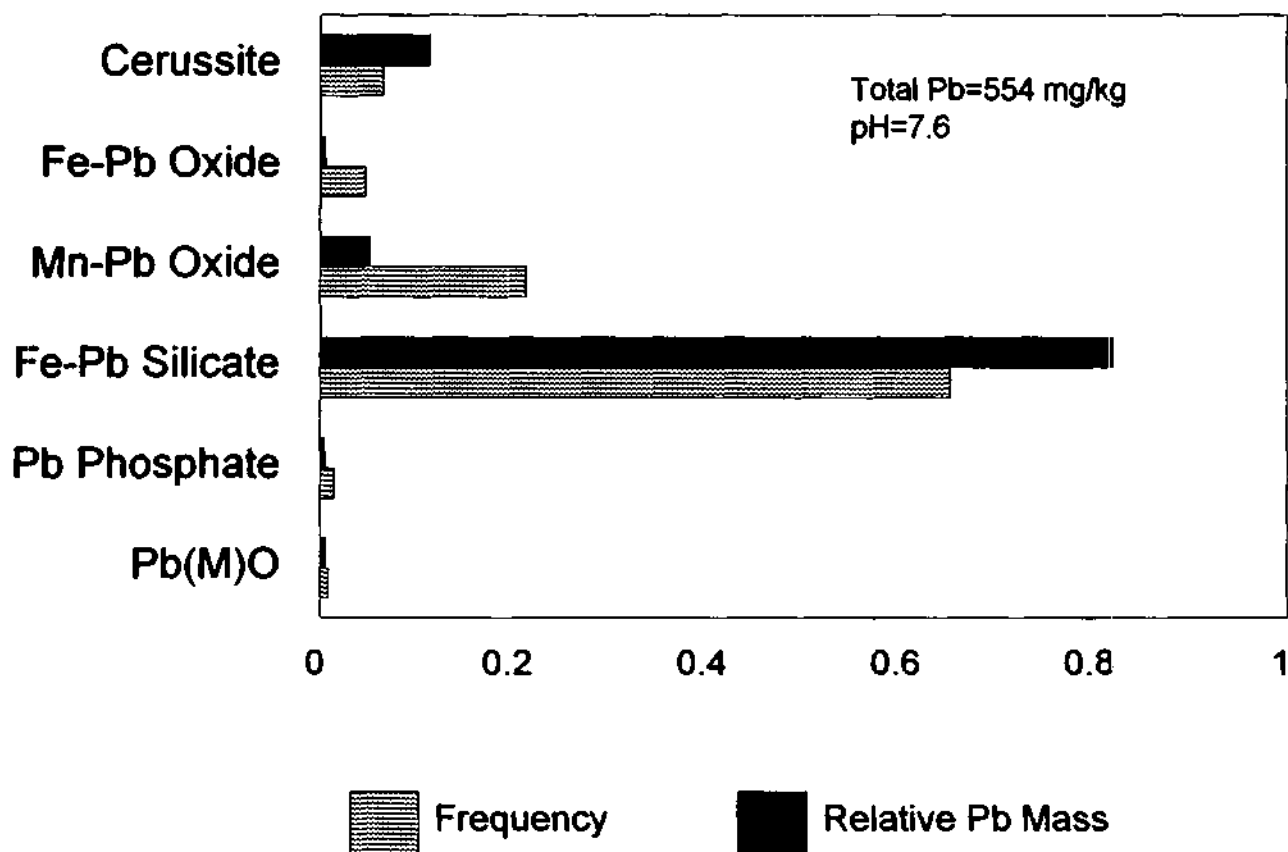


Figure 12. Frequency and Relative Pb Mass of Pb Phases in Undisturbed Alluvium.

Rico, Colorado

Lab Sample SOO1576

(Field Sample #940)

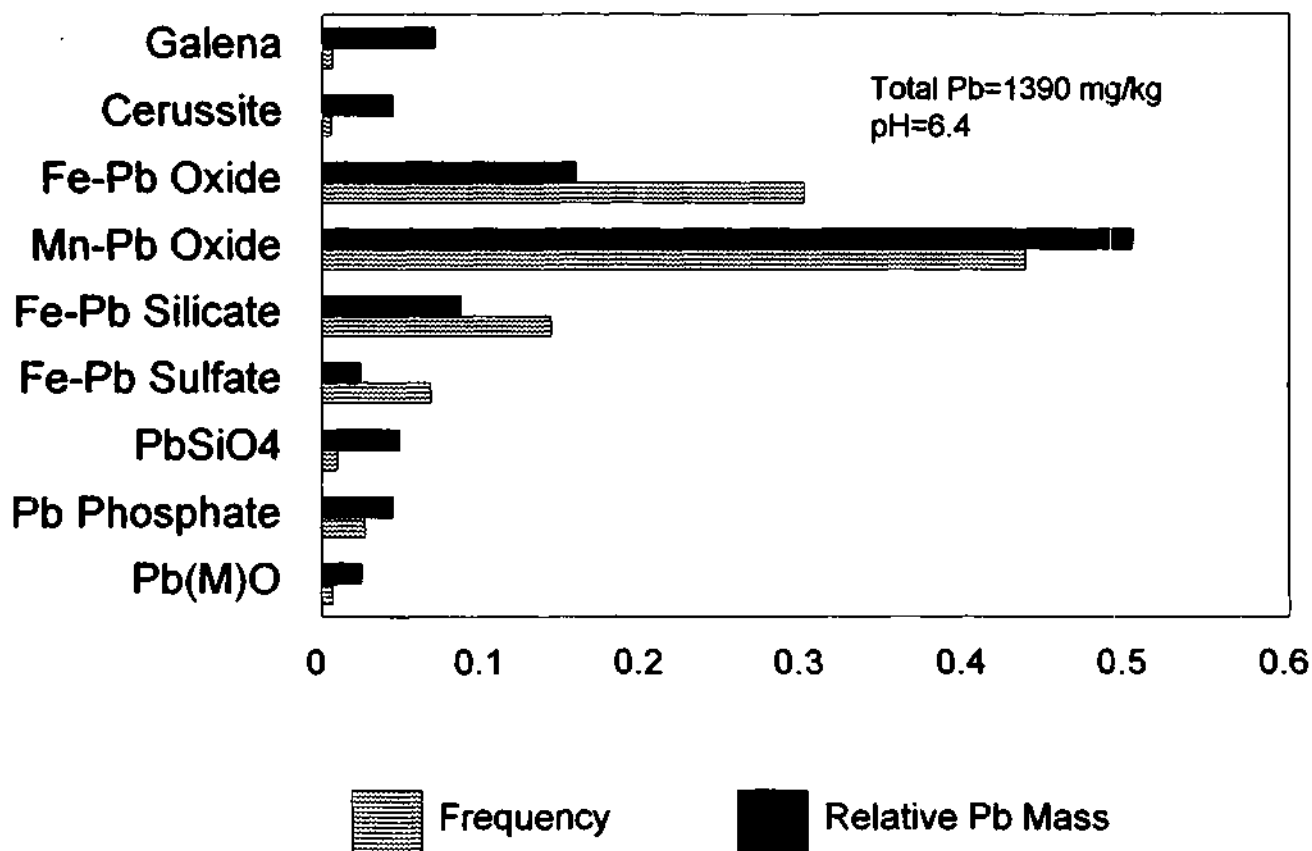


Figure 13. Frequency and Relative Pb Mass of Pb Phases in Disturbed Colluvium.

Rico, Colorado

Lab Sample SOO1579
(Field Sample #943)

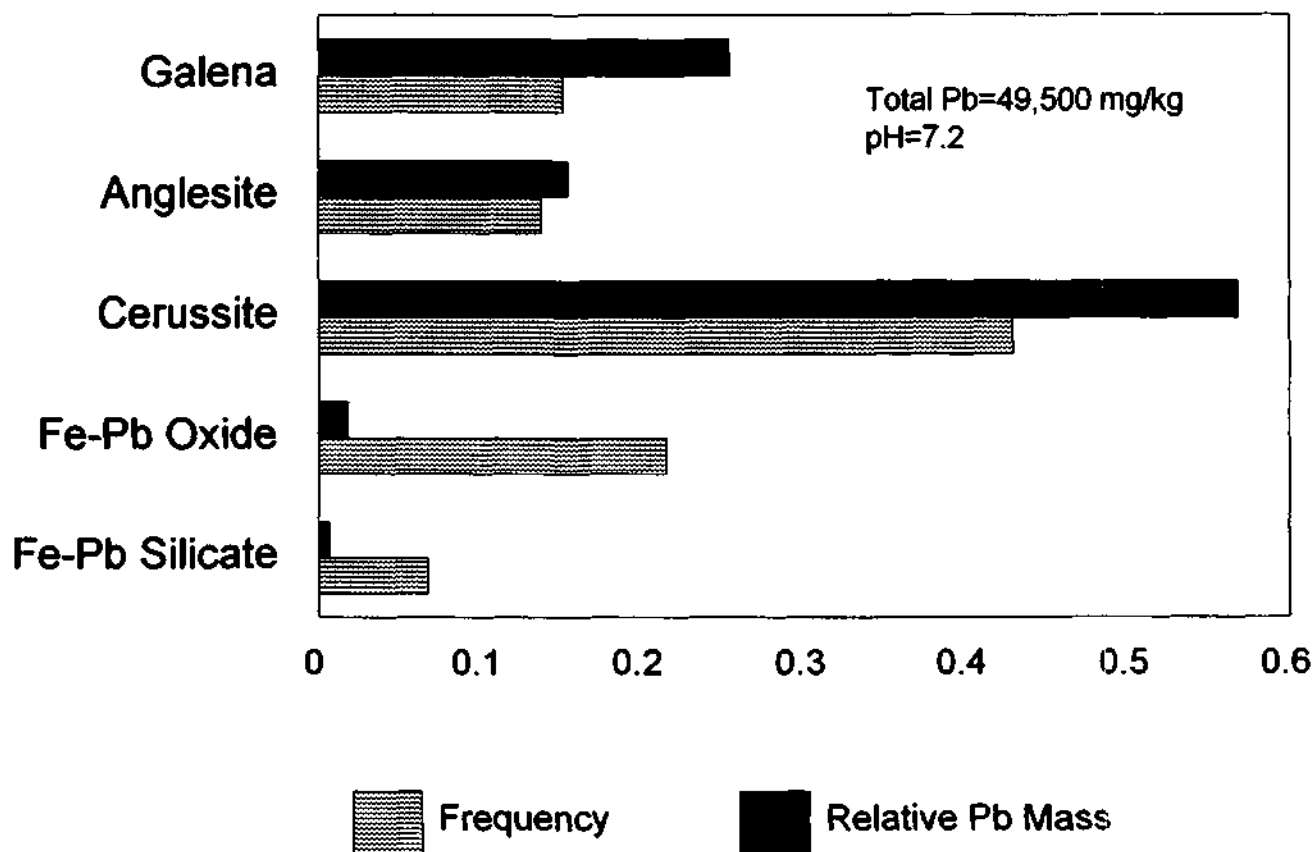


Figure 14. Frequency and Relative Pb Mass of Pb Phases in Undisturbed Colluvium.

Rico, Colorado

Lab Sample SOO1581
(Field Sample #945)

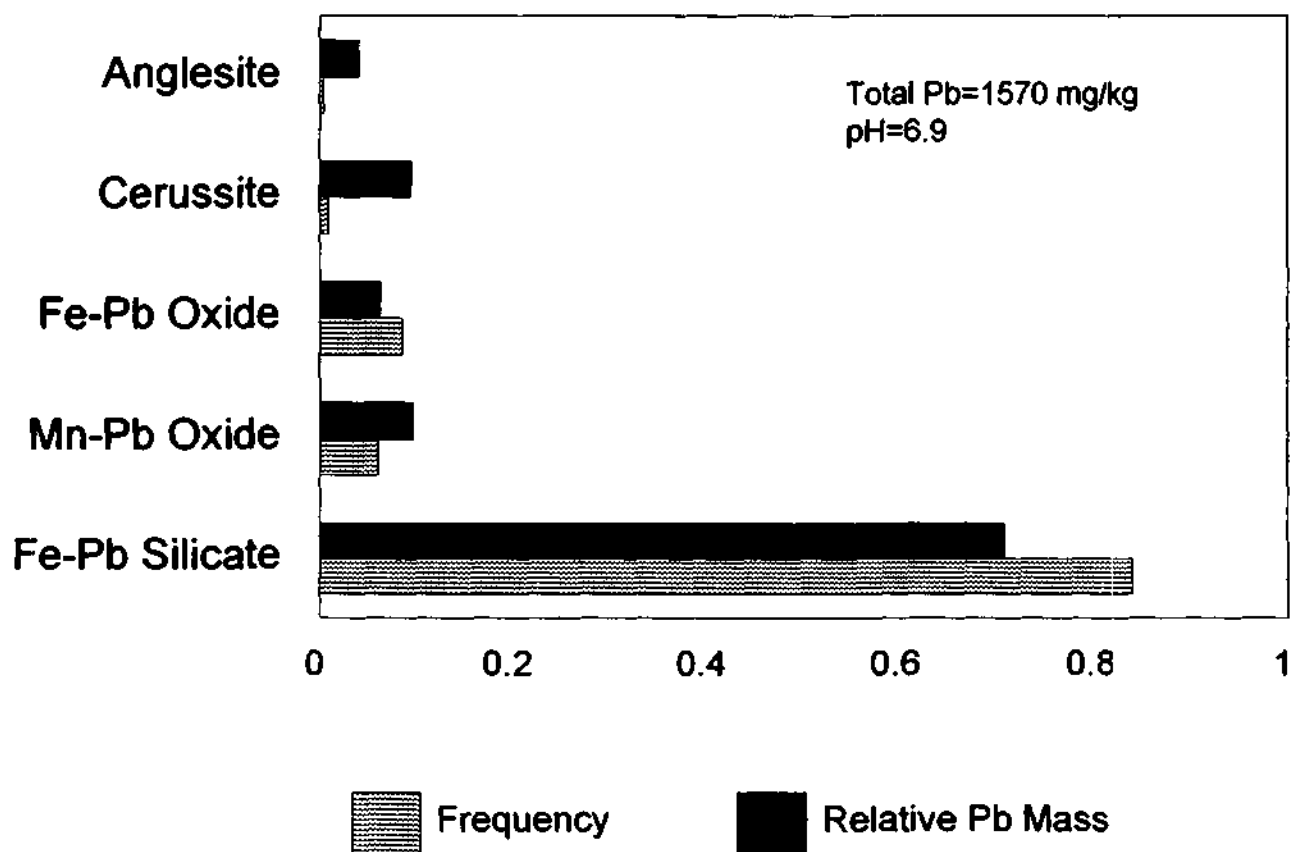


Figure 15. Frequency and Relative Pb Mass of Pb Phases in Undisturbed Colluvium.

Rico, Colorado

Lab Sample SOO1919
(Field Sample #96-CH-01)

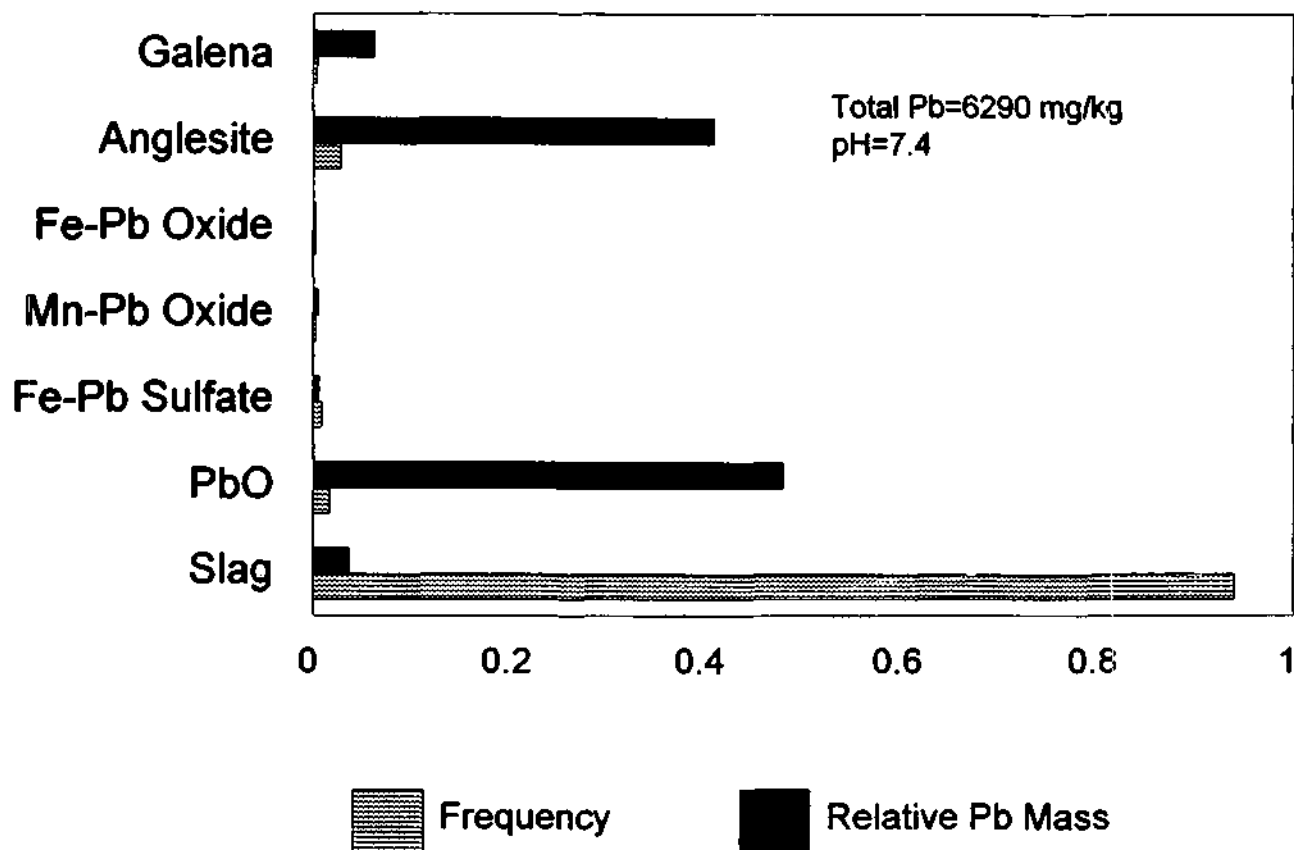


Figure 16. Frequency and Relative Pb Mass of Pb Phases in Grand View Smelter Sample.

Rico, Colorado

Lab Sample SOO1920

(Field Sample #96-CH-02)

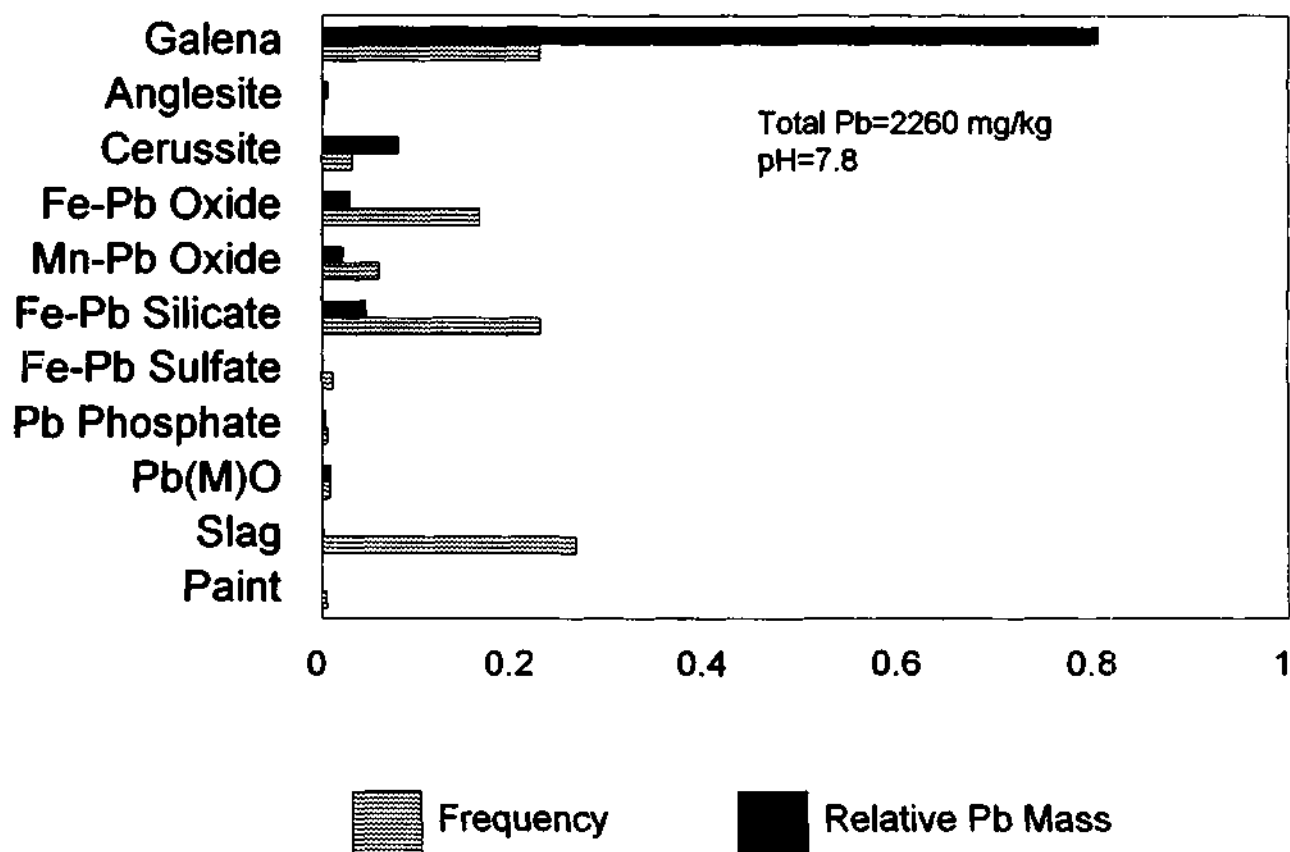


Figure 17. Frequency and Relative Pb Mass of Pb Phases in Roadfill Material.

Rico, Colorado

Lab Sample SOO1921
(Field Sample #96-CH-03)

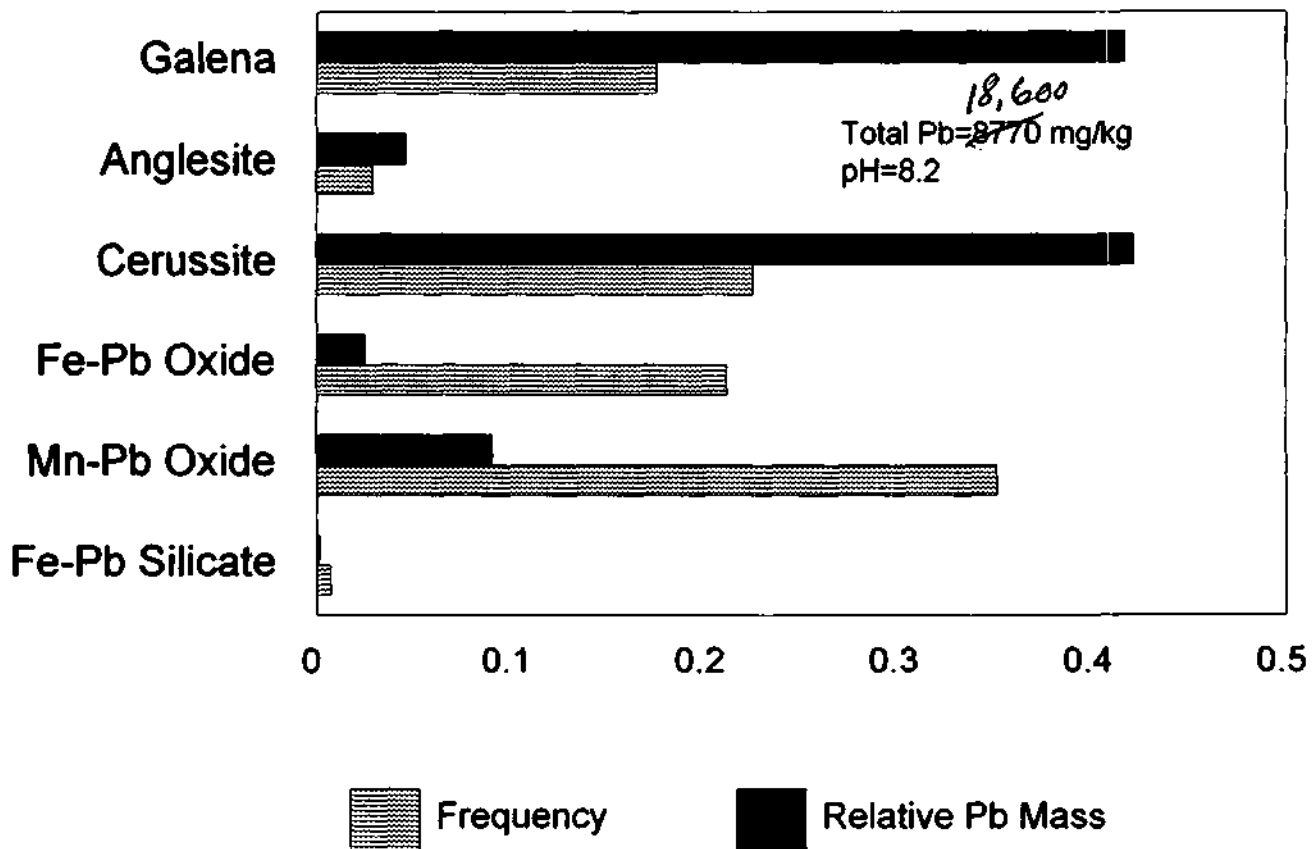


Figure 18. Frequency and Relative Pb Mass of Pb Phases in Van Winkle Mine Waste Rock.

Rico, Colorado

Lab Sample SOO1922
(Field Sample #96-CH-04)

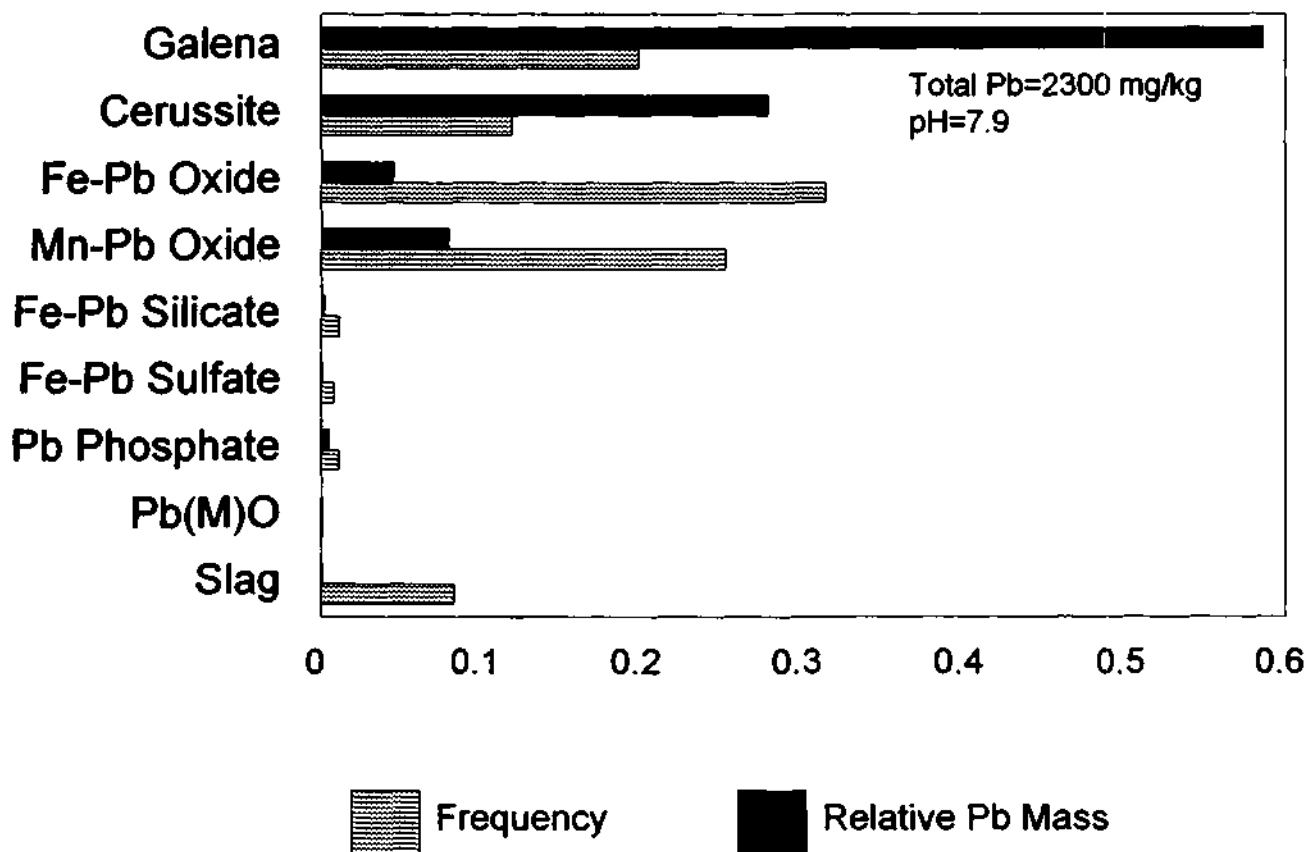


Figure 19. Frequency and Relative Pb Mass of Pb Phases in Roadfill Material.



Figure 2-20 . Photomicrograph showing paragenetic relationship between primary Pb phase (galena-PbS) and secondary Pb phases (anglesite-PbSO₄ and cerussite-PbCO₃). Galena oxidizes directly to PbSO₄ which then converts to PbCO₃ in response to alkaline pH conditions (Sample is from Van Winkle mine site)



Figure 2-21 . Photomicrograph of tertiary phase MnPb oxide precipitate encapsulating secondary phase PbCO_3 grains. As PbCO_3 is subjected to dissolution, Pb^{2+} ions are scavenged and coprecipitated by Mn oxides. (Sample is from 6-8' depth in Quarternary alluvium).

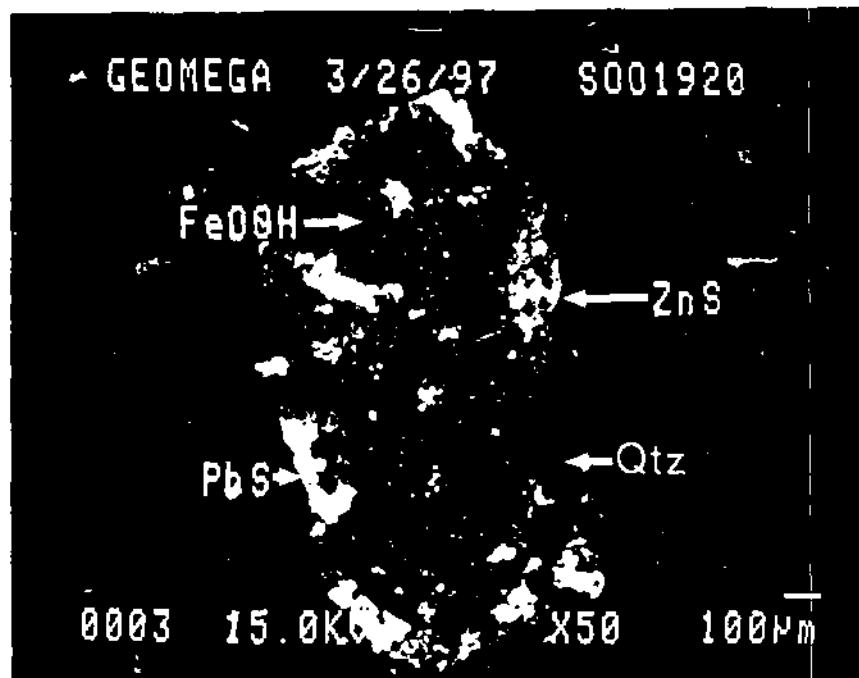


Figure 22. Photomicrograph of composite grain of FeOOH hosting primary mineral sulfides (galena-PbS and sphalerite-ZnS) and quartz. Dissolution of PbS supplies Pb^{2+} ions that are adsorbed and coprecipitated with Fe and Mn as amorphous oxide and silicate solid phases. (Sample is from roadfill material).